Anaplasma phagocytophilum induces actin phosphorylation to selectively regulate gene transcription in *Ixodes scapularis* ticks

Hameeda Sultana,[1,5] Girish Neelakanta,[1] Fred S. Kantor,[2] Stephen E. Malawista,[3] Durland Fish,[4] Ruth R. Montgomery,[3] and Erol Fikrig[1,5]

[1]Section of Infectious Diseases, [2]Section of Allergy and Clinical Immunology, [3]Section of Rheumatology, Department of Internal Medicine, and [4]Department of Epidemiology and Public Health, Yale University School of Medicine, New Haven, CT 06520
[5]Howard Hughes Medical Institute, Chevy Chase, MD 20815

Anaplasma phagocytophilum, the agent of human anaplasmosis, persists in ticks and mammals. We show that *A. phagocytophilum* induces the phosphorylation of actin in an *Ixodes ricinus* tick cell line and *Ixodes scapularis* ticks, to alter the ratio of monomeric/filamentous (G/F) actin. *A. phagocytophilum*–induced actin phosphorylation was dependent on *Ixodes* p21–activated kinase (IPAK1)–mediated signaling. *A. phagocytophilum* stimulated IPAK1 activity via the G protein–coupled receptor Gβγ subunits, which mediated phosphoinositide 3-kinase (PI3K) activation. Disruption of *Ixodes gβγ*, *pi3k*, and *pak1* reduced actin phosphorylation and bacterial acquisition by ticks. *A. phagocytophilum*–induced actin phosphorylation resulted in increased nuclear G actin and phosphorylated actin. The latter, in association with RNA polymerase II (RNAPII), enhanced binding of TATA box–binding protein to RNAPII and selectively promoted expression of *salp16*, a gene crucial for *A. phagocytophilum* survival. These data define a mechanism that *A. phagocytophilum* uses to selectively alter arthropod gene expression for its benefit and suggest new strategies to interfere with the life cycle of this intracellular pathogen, and perhaps other *Rickettsia*-related microbes of medical importance.

CORRESPONDENCE
Erol Fikrig:
erol.fikrig@yale.edu

Abbreviations: DNAP, DNA affinity precipitation; EMSA, electrophoretic mobility shift assay; *ipak1*, *Ixodes pak1*; *ipi3k*, *Ixodes pi3k*; LC-MS/MS, liquid chromatography–tandem mass spectrometry; MBP, myelin basic protein; PAK1, p21-activated kinase; PBD, p21-binding domain of PAK1; PI3K, phosphoinositide 3-kinase; RNAPII, RNA polymerase II; TBP, TATA box–binding protein.

Human Granulocytic Anaplasmosis is an increasingly common tick-borne illness in the United States, Europe, and Asia (Dumler et al., 2005; Bakken and Dumler, 2008). The agent of this disease, *Anaplasma phagocytophilum*, survives within human neutrophils using several strategies, including delaying apoptosis, inhibiting NADPH oxidase activity, and subverting phagolysosome biogenesis to reside in an inclusion that does not fuse with lysosomes (Carlyon and Fikrig, 2003). Tyrosine phosphorylation of translocated bacterial effector proteins is another key feature that enables pathogens to thwart host cell signaling (Selbach et al., 2009). Several proteins translocated by bacterial type III and IV secretion systems are involved in pedestal formation (Tir of *EPEC and Citrobacter*), cell scattering (CagA of *Helicobacter*), invasion (Tarp of *Chlamydia*), and cell proliferation (BepD-F of Bartonella; Covacci and Rappuoli, 2000). Bacterial protein tyrosine kinases and

phosphatases also play a role in pathogenicity and enable the microbe to short circuit host defense mechanisms and thwart signaling (Covacci and Rappuoli, 2000). *A. phagocytophilum* AnkA protein is tyrosine phosphorylated by Abl-1 kinase to facilitate infection (Lin et al., 2007; IJdo et al., 2007). *A. phagocytophilum* AnkA also binds to granulocyte DNA and nuclear proteins, leading to speculation about the functional nature of AnkA–host cell DNA interactions (Park et al., 2004). The agent of human granulocytic anaplasmosis also induces the tyrosine phosphorylation of ROCK1 in human neutrophils to aid in intracellular survival (Thomas and Fikrig, 2007). Collectively, these studies demonstrate that this unique obligate intracellular pathogen has evolved diverse mechanisms to persist within mammalian cells and that tyrosine phosphorylation of proteins

---

H. Sultana and G. Neelakanta contributed equally to this paper.

plays an important role in the manipulation of host cellular events to promote *A. phagocytophilum* survival.

A. phagocytophilum is closely related to other arthropod-borne bacteria in the genera *Rickettsia* and *Ehrlichia* that infect the mammalian host (Dumler et al., 2001). Intracellular microorganisms, including *Rickettsia*, *Shigella*, *Listeria*, and vaccinia virus, among others, use actin polymerization to move within and spread between cells (Frischknecht et al., 1999a; Goosney et al., 1999; Gouin et al., 2004; Cossart and Toledo-Arana, 2008). These pathogens recruit host actin and cytoskeletal proteins to their surface and activate the assembly of an actin comet tail (Goldberg, 2001; Gouin et al., 2005; Cossart and Toledo-Arana, 2008). In contrast, *Salmonella*, *Neisseria*, and *Bartonella* intercept actin rearrangements during internalization (Dramsi and Cossart, 1998; Patel and Galán, 2005; Patel et al., 2009). Some microbes manipulate the actin cytoskeleton by directly injecting effectors or virulence factors into cells, thereby specifically targeting crucial intracellular signaling pathways (Sansonetti, 2002; Münter et al., 2006; Bhavsar et al., 2007). *Yersinia* activates the effector protein YpkA to phosphorylate Gαq and cause the disassembly of actin stress fibers (Navarro et al., 2007). Vaccinia virus achieves actin-based motility by mimicking the tyrosine kinase signaling pathways that control actin nucleation dynamics (Frischknecht et al., 1999b). In mammalian cells, the *Rickettsia* surface protein RickA activates the Arp2/3 complex to induce actin polymerization and filopodia formation (Martinez and Cossart, 2004). The essential role of actin-based motility and actin dynamics has not been examined in the arthropod vector.

Some bacteria use arthropod components and signaling events to survive in the vector or to facilitate transmission to the host. *A. phagocytophilum* is naturally maintained in a tick-rodent cycle. Humans are merely incidental hosts. Uninfected *Ixodes scapularis* larvae acquire *A. phagocytophilum* within 2 d of tick engorgement on *A. phagocytophilum*–infected mice, and once in the tick, the bacteria migrate through the gut to infect the salivary glands (Hodzic et al., 1998). The larvae molt into nymphs and later into adults, whereas the bacteria persist within the secretory acini of the salivary glands (Hodzic et al., 1998; Katavolos et al., 1998). Upon tick feeding, the bacteria replicate and migrate from the salivary glands to the mammalian host (to invade granulocytes), and the transmission of *A. phagocytophilum* occurs between 24 and 48 h after tick engorgement (Hodzic et al., 1998; Katavolos et al., 1998). *I. scapularis*, the black-legged tick, is a vector for viral and bacterial pathogens including *A. phagocytophilum* and *Borrelia burgdorferi*, the agent of Lyme disease (Schwan, 1996; Dumler et al., 2005). The extended period of association of these microbes with the vector has resulted in the development of intimate relationships between pathogen and arthropod. For example, *B. burgdorferi* uses Salp15, a tick salivary gland protein, to facilitate infection of the mammalian host (Ramamoorthi et al., 2005). Salp15 is selectively increased in *B. burgdorferi*–infected tick salivary glands during engorgement, and silencing of the *salp15* gene in *I. scapularis* reduced the capacity of tick-borne spirochaetes to infect mice (Ramamoorthi et al., 2005). In addition, Salp15

binds *B. burgdorferi*, thereby protecting the spirochete from antibody-mediated killing (Ramamoorthi et al., 2005). *A. phagocytophilum* up-regulates Salp16, a tick salivary gland protein, to survive in its arthropod vector (Sukumaran et al., 2006). Acquisition of *A. phagocytophilum* from the infected mammalian host was severely inhibited and the bacterial loads were substantially lower in the salivary glands of *salp16*-silenced ticks, thereby suggesting that *A. phagocytophilum* specifically requires *salp16* to infect salivary glands (Sukumaran et al., 2006). When Salp16 is not present in *I. scapularis*, as demonstrated in RNAi studies, *A. phagocytophilum* can no longer effectively persist within tick salivary glands (Sukumaran et al., 2006). The mechanisms used by *A. phagocytophilum* to influence its arthropod vector, including the expression of *I. scapularis* genes, are not known. We now explore whether *A. phagocytophilum* selectively modulates arthropod signaling by altering protein phosphorylation and whether these processes influence *I. scapularis* gene expression and survival of *A. phagocytophilum* within ticks.

RESULTS

A. phagocytophilum induces phosphorylation of tick actin

The tyrosine phosphorylation of *Ixodes* proteins upon *A. phagocytophilum* infection was first examined using an *Ixodes ricinus* tick cell line (Bell-Sakyi et al., 2007). Immunofluorescence showed increased phosphorylation of proteins in *A. phagocytophilum*–infected cells in comparison with the uninfected controls (Fig. 1 A). Although the phosphotyrosine signal was more localized to the periphery and filamentous filopodial structures in uninfected cells, *A. phagocytophilum*–infected cells showed an irregular distribution of the phosphorylated proteins as large clusters (Fig. 1 A). Immunoblotting demonstrated that *A. phagocytophilum* markedly induced phosphorylation of a major *Ixodes* protein (Fig. 1 B and Table S1) that was identified as actin by mass spectrometry analysis. Actin was shown to be heavily phosphorylated at residue Y53 (Jungbluth et al., 1995). The tyrosine residue (Y53) is also conserved in *I. scapularis* actin (National Center for Biotechnology Information [NCBI] protein accession no. XP_002408110). However, the liquid chromatography–tandem mass spectrometry (LC-MS/MS) phosphopeptide identification results revealed that the peptide LCYVALDFEQEMATAASSSSLEK contained the phosphosite and that tyrosine residue corresponds to Y178 of *I. scapularis* actin (NCBI protein accession no. XP_002408110). Immunoprecipitation of a tick cell extract with phosphotyrosine antibody, followed by immunoblotting with actin antibody, confirmed that *A. phagocytophilum* induces phosphorylation of actin (Fig. 1 C and Table S1). We also found that *A. phagocytophilum* induces the threonine but not serine phosphorylation of actin (Fig. S1, A snd B; and Table S1).

To determine the temporal development of *A. phagocytophilum*–induced phosphorylation of actin, tick cells were analyzed over 10 d. Phosphorylation was evident at 24 h and persisted through day 10 (Fig. 1 D and Table S1). *A. phagocytophilum* infection was apparent at all time points during the course of infection (Fig. 1 E). The infection rate of *A. phagocytophilum* in
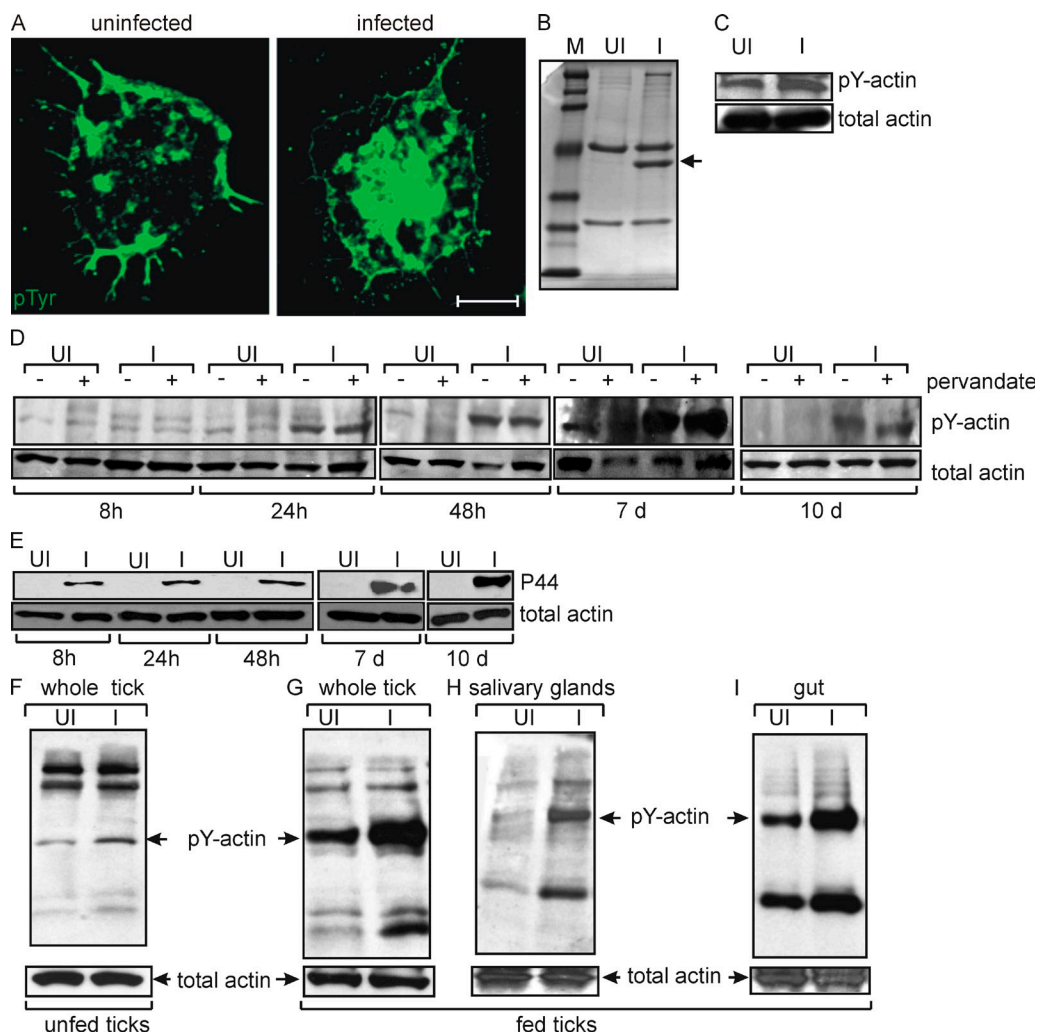
Figure 1.   *A. phagocytophilum* induces actin phosphorylation in tick cells and ticks. (A) Immunofluorescence images of uninfected and *A. phagocytophilum*–infected tick cells at 48 h after infection, stained for phosphotyrosine (pTyr). Bar, 10 µm. Representative images are shown from three independent experiments. (B) Coomassie-stained SDS-PAGE image of anti-pTyr immunoprecipitated proteins from uninfected (UI) and *A. phagocytophilum*–infected (I) lysates at 48 h after infection. The arrow denotes the dominant phosphorylated band identified as actin in *A. phagocytophilum*–infected cells. Phosphorylation of a protein with a higher molecular mass was also noted. (C) Lysates with (I) or without (UI) *A. phagocytophilum* were immunoprecipitated with antibodies against pTyr and probed with antibodies against actin. The level of actin before immunoprecipitation (total actin) served as the loading control. (D) Lysates from cells infected (I) or not (UI) with *A. phagocytophilum* were isolated at different time points (8, 24, and 48 h and 7 and 10 d) and assessed for actin phosphorylation in the presence (+) or absence (−) of pervanadate, a protein tyrosine phosphatase inhibitor. (E) The presence of *A. phagocytophilum* in infected tick cells was assessed by immunoblotting with antisera specific for the *A. phagocytophilum* P44 antigen (P44). Actin served as loading control. (F) Lysates were prepared from unfed ticks infected (I) or not (UI) with *A. phagocytophilum*. 20 µg of total lysates were probed with pTyr-specific antibody. pY-actin is denoted by an arrow. Total actin served as loading control. Whole tick (G), salivary gland (H), and gut tissue (I) lysates were prepared from *I. scapularis* fed for 48 h on uninfected or *A. phagocytophilum*–infected mice and were analyzed as described in F. Representative data are shown from three independent experiments in all panels.

tick cells was found to be 70 ± 9% (Fig. S1, C and D). To determine whether inhibition of protein tyrosine phosphatases altered *A. phagocytophilum*–induced extended actin phosphorylation, tick cells were treated with pervanadate, a protein tyrosine phosphatase inhibitor. Actin phosphorylation was comparable in pervanadate-treated and untreated *A. phagocytophilum*–infected cells (Fig. 1 D), suggesting that inhibition of tick tyrosine phosphatase activity did not influence *A. phagocytophilum*–induced actin phosphorylation.

A. phagocytophilum induces phosphorylation of actin in unfed ticks and during acquisition by ticks

To assess whether actin phosphorylation occurs in vivo, the phosphorylation pattern in *A. phagocytophilum*–infected ticks was examined. Actin phosphorylation was induced in *A. phagocytophilum*–infected unfed nymphs in comparison with the uninfected controls, suggesting an extended and stable modification of actin (Fig. 1 F and Table S1). Immunofluorescence of unfed tick salivary glands also demonstrated elevated

levels of phosphorylated actin upon *A. phagocytophilum* infection (Fig. S1 E). To examine whether acquisition of *A. phagocytophilum* by ticks induces actin phosphorylation, uninfected nymphs were fed on either *A. phagocytophilum*–infected or uninfected mice. Ticks were collected at 24, 48, and 72 h during engorgement and at 48 and 72 h after feeding. Actin phosphorylation was evident at all time points examined (data at 48 h during feeding are shown; Fig. 1 G and Table S1). An elevated level of a phosphorylated protein with a lower molecular mass was also seen in *A. phagocytophilum*–infected ticks compared with the uninfected controls. *A. phagocytophilum*–induced actin phosphorylation was then specifically assessed in the tick gut, the site of microbial entry, and the salivary glands, the site of pathogen persistence. After 48 h of engorgement, *A. phagocytophilum*–induced actin phosphorylation was significantly increased (2.6–4.0 fold) in the tick salivary glands and gut (Fig. 1, H and I; and Table S1), suggesting that *A. phagocytophilum*–induced actin phosphorylation occurs in both these tissues.

A. phagocytophilum–induced actin phosphorylation is mediated by phosphoinositide 3–kinase (PI3K)– p21–activated kinase (PAK1) signaling
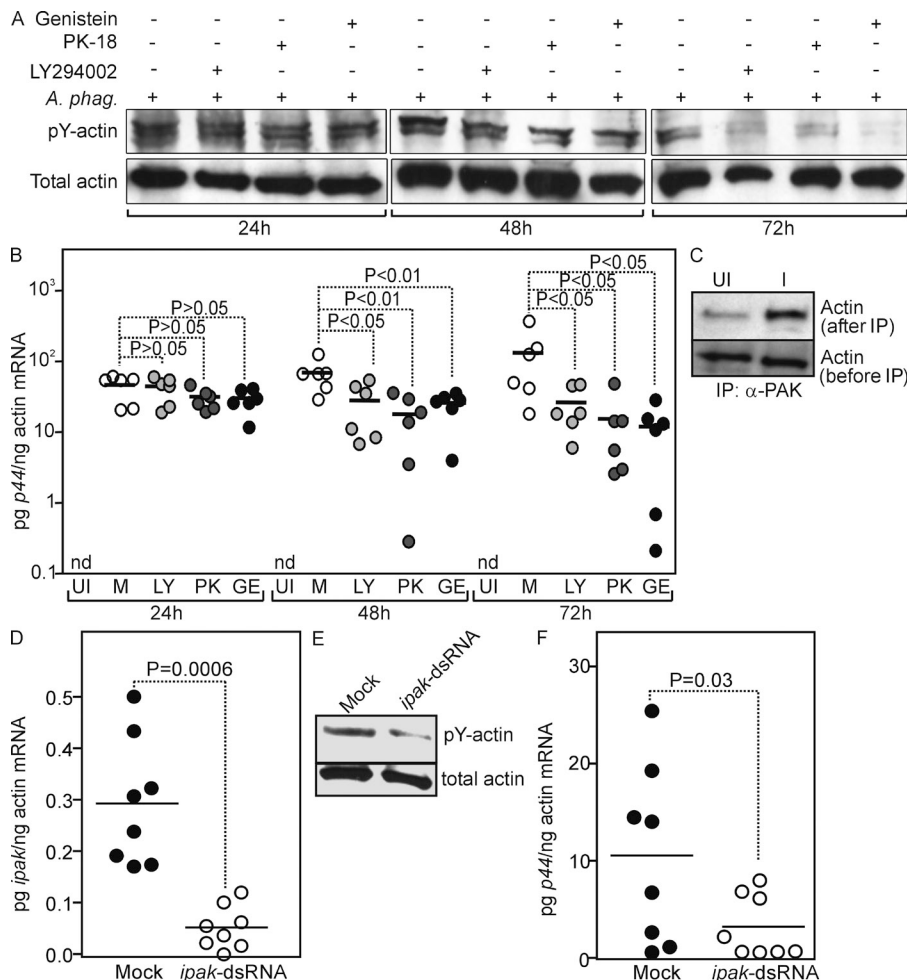
Studies in *Drosophila melanogaster* have shown that PAK1 plays an important role in linking to tyrosine kinase signaling pathways through Dock (Nck homologue), thereby leading to changes in the reorganization of the actin cytoskeleton (Galisteo et al., 1996). The adaptor protein Nck has also been shown to directly couple PAK1 signaling to receptor tyrosine kinases in several mammalian tissue culture systems (McCarty, 1998). Furthermore, the association of PI3K and PAK1 phosphorylates actin and reorganizes the actin cytoskeleton in an opossum kidney epithelial cell line (Papakonstanti and Stournaras, 2002). These studies suggest PI3K-PAK1 signaling to be a central component in actin phosphorylation. To characterize whether these kinases are regulating *A. phagocytophilum*–induced phosphorylation of actin, we searched the *I. scapularis* genome database and identified partial coding sequences for both of these genes as described in the Materials and methods. We designated the tick PI3K as *Ixodes pi3k* (*ipi3k*) and PAK1 as *Ixodes pak1* (*ipak1*). The GenBank accession nos. for *ipi3k* and *ipak1* are HM165193 and HM165194, respectively. The *I. scapularis* IPI3K and IPAK1 homologues (Fig. S2, A and B) showed high similarity (80–85%) and identity (65–70%) to the PI3K and PAK1 proteins from *Drosophila melanogaster*, *Aedes aegypti*, mice, and man (Fig. S3, A and B). G protein–coupled receptor Gβγ subunits stimulate PAK1 through activation of PI3K but act independently of Rac1/ Cdc42 GTPases (Menard and Mattingly, 2004). We found the annotated coding sequences for both the Gβ (accession no. XP_002401352) and Gγ subunits (accession no. EEC12500) from the NCBI Protein database. In the current study, we designated the tick G protein–coupled receptor β subunit as *igβ* and the γ subunit as *igγ*. The *I. scapularis* Gβ and Gγ homologues showed 55 and 44% amino acid identity, respectively, to Gβ1 and Gγ2 in humans (Fig. S4, A and B).

We found that the expression of *ipak1*, *ipi3k*, and both *igβ* and *igγ* were significantly elevated in *A. phagocytophilum*–infected unfed ticks and in uninfected ticks that acquired *A. phagocytophilum* from infected mice (Fig. S5, A–H). These data suggest that *A. phagocytophilum* elevates the expression of the G protein–coupled receptor Gβγ subunits, which leads to activation of the PI3K–PAK1 signaling pathways.

To study whether inhibition of *ipi3k*, *ipak1*, or tyrosine kinases affects *A. phagocytophilum*–induced actin phosphorylation, we infected tick cells with *A. phagocytophilum* and simultaneously treated them with LY294002 (an inhibitor of PI3K), PK-18 (a potent PAK1 inhibitor), or Genistein (a protein tyrosine kinase inhibitor). At 48 and 72 h, cells treated with each of the three inhibitors showed a considerable reduction in actin phosphorylation (Fig. 2 A and Table S1) and a significant decrease in the *A. phagocytophilum* burden (Fig. 2 B) in comparison with the controls. To study whether these inhibitors reduced actin phosphorylation and the bacterial load in vivo, we performed microinjections of these inhibitors into *A. phagocytophilum*–infected nymphs. At 24 h, we found a considerable reduction in actin phosphorylation in *A. phagocytophilum*–infected unfed ticks when compared with the mock controls (Fig. S5 I and Table S1). During acquisition of *A. phagocytophilum* by ticks, actin phosphorylation and bacterial loads were also significantly reduced in PK-18 or Genistein inhibitor-treated ticks at 48 h after engorgement (Fig. S5, J and K; and Table S1).

Silencing of *ipak1* reduces actin phosphorylation and *A. phagocytophilum* acquisition by ticks

To establish the interaction of tick IPAK1 with actin, we performed immunoprecipitation studies of control and *A. phagocytophilum*–infected tick cells. Immunoblots performed with mammalian PAK1 antibody demonstrated specific cross-reactivity with IPAK1 (Fig. S5L, Table S1). When we immunoprecipitated IPAK1, immunoblotting with actin antibody demonstrated a direct and conserved in vivo association between IPAK1 and actin. Moreover, the interaction between IPAK1 and actin was enhanced upon *A. phagocytophilum* infection (Fig. 2 C and Table S1), suggesting an important role for IPAK1 in inducing actin phosphorylation. To examine whether IPAK1 plays a specific role in the acquisition of *A. phagocytophilum* by ticks, *ipak1*-deficient nymphs were produced by RNAi treatment. At 48 h of engorgement, the level of *ipak1* mRNA was significantly decreased in the *ipak1*-dsRNA–injected groups and, concomitantly, *A. phagocytophilum*–induced tyrosine phosphorylation of actin was substantially reduced in *ipak1*-dsRNA–injected ticks (Fig. 2, D and E; and Table S1). The reduction in threonine phosphorylation of actin was also evident in *ipak*-dsRNA–injected ticks in comparison with the mock controls (Fig. S6 A and Table S1). The *A. phagocytophilum* burden in the *ipak1*-dsRNA–injected group was also markedly diminished when compared with the controls (Fig. 2 F). These data further suggest that IPAK1 signaling and actin phosphorylation are required for *A. phagocytophilum* survival in ticks.

Figure 2. Ixodes PI3K, PAK1, or tyrosine kinases affect A. phagocytophilum–induced actin phosphorylation and bacterial loads in tick cells. (A) Tick cells treated with PI3K (LY294002), PAK1 (PK-18), or tyrosine kinase (Genistein) inhibitors were infected with *A. phagocytophilum* (*A. phag.*) and assessed for actin phosphorylation at 24, 48, and 72 h. Phosphorylated (pY-actin) and total actin (loading control) were analyzed by probing with pTyr-specific and actin-specific antibodies, respectively. Mock samples were treated with equal amounts of DMSO. Representative data from two independent experiments is shown. (B) *A. phagocytophilum* burden in tick cells was measured by quantifying *p44* mRNA levels normalized against tick *β actin* mRNA. UI, uninfected; M, mock; LY, PI3K-inhibitor; PK, PAK1-inhibitor; GE, Genistein; nd, nondetectable. Each circle represents one independent experiment. (C) Whole infected (I) or uninfected (UI) tick cell extracts were immunoprecipitated (IP) with PAK1-specific antibody and immunoblotted for actin. Total cell lysates (before immunoprecipitation) probed with actin-specific antibody served as the loading control. (D) Q-RT-PCR showing reduced *ipak1* mRNA levels in *ipak1*-dsRNA–injected ticks compared with the mock controls (buffer alone). Each circle represents one tick. (E) Phosphorylated (pY-actin) and total actin levels (loading control) from tick lysates were analyzed by immunoblotting with pTyr-specific and actin-specific antibodies, respectively. (F) The *A. phagocytophilum* burden in ticks was measured by quantifying *p44* mRNA levels normalized against tick *β actin* mRNA. Each circle represents an individual tick. Statistics were performed using the Student's *t* test and the p-value is shown. Representative data from three independent experiments is shown. Horizontal bars in B, D, and F indicate mean values of the data points.

A. phagocytophilum induces IPAK1 activity through IPI3K activation

To determine whether *A. phagocytophilum*-induced actin phosphorylation was dependent on IPAK1 activation, total lysates from the 48 h during tick feeding were immunoprecipitated with PAK1 antibody. IPAK1 activation was examined by determining the phosphorylation of myelin basic protein (MBP), a known exogenous substrate for PAK1 activity. We found that *A. phagocytophilum* induces strong activation of IPAK1 (Fig. 3 A and Table S1). Total lysates used for immunoprecipitation of IPAK1 (input) were probed with actin antibody as the loading control (Fig. 3 A). The association of PI3K with PAK1 regulates PAK1 activity (Papakonstanti and Stournaras, 2002). We found that *A. phagocytophilum* also induces IPI3K activity, as determined by the generation of phosphatidylinositol-3,4,5-triphosphate PI(3)P from phosphatidylinositol (Fig. 3 B). We therefore generated *ipi3k*-deficient *A. phagocytophilum*–infected ticks. The level of *ipi3k* mRNA and the *A. phagocytophilum* burden were significantly reduced in the *ipi3k*-dsRNA–injected groups when compared

with the mock controls (Fig. S6, B and C). Furthermore, *A. phagocytophilum*–induced tyrosine phosphorylation of actin was markedly diminished in *ipi3k*-dsRNA–injected ticks (Fig. S6 D and Table S1), suggesting an important role for the association of PI3K with PAK1 in actin phosphorylation. We then examined the IPAK1 activity in mock or *ipi3k*-dsRNA–treated ticks by immunoprecipitation of IPAK1. IPAK1 kinase activity was dramatically reduced in *ipi3k*-deficient ticks when compared with the mock controls (Fig. 3 C and Table S1).

A. phagocytophilum–induced IPAK1 activity is dependent on Gβγ stimulation but independent of Rac1/Cdc42 activation

Heterotrimeric G proteins have been implicated in PAK1 and PI3K activation (Menard and Mattingly, 2004). The *A. phagocytophilum*–induced expression of *igβ* and *igγ* (Fig. S5, E–H) prompted us to investigate the upstream mechanisms. Silencing of *igβ* and *igγ* (Fig. S6, E and F) decreased the *A. phagocytophilum* burden (Fig. S6, G and H) and reduced the tyrosine phosphorylation of actin (Fig. S6 I and Table S1). IPAK1 and IPI3K activities were dramatically reduced in both
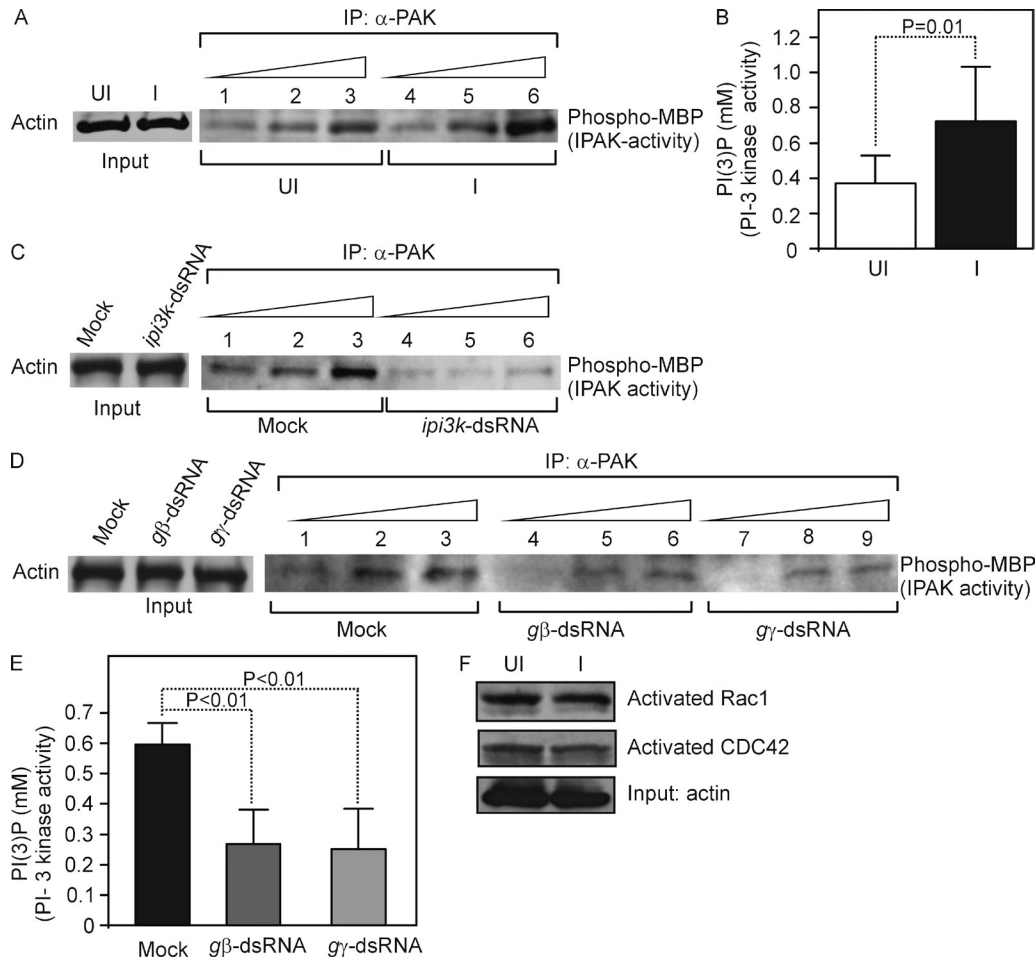
Figure 3. *A. phagocytophilum* infection induces IPAK1 and IPI3K activity through Gβγ stimulation but independent of Rac1/Cdc42 activation. (A) Lysates from ticks infected (I) or not (UI) with *A. phagocytophilum* were immunoprecipitated (IP) with anti-PAK1, and PAK1-mediated phosphorylation of the substrate MBP was analyzed by in vitro kinase assay. Total lysates used for the kinase assay were probed with actin antibody as the loading control (input). (B) IPI3K activity read out by ELISA detecting PI conversion to PI(3)P, IPI-3 immunoprecipitates from lysates of *A. phagocytophilum*–infected or uninfected ticks. (C and D) IPAK1 activity in *ipi3k*-silenced ticks (C) or *igβ*- or *igγ*-silenced ticks (D) in comparison with their respective mock controls was measured as in A. Total lysates used for the kinase assays were probed with actin antibody as the loading control. In A, C, and D, IPAK immunoprecipitates were used at three different dilutions indicated by wedges (10, 15, and 25 μl IP beads). (E) IPI3K activity in *igβ*- or *igγ*-silenced ticks in comparison with the mock control was determined as in B. (F) Rac1/Cdc42 activation upon binding to PAK-PBD (Rac1/CDC42 binding domain of PAK1) upon *A. phagocytophilum* infection. Total tick lysates were used for affinity precipitation of Rac1/Cdc42 GTPases with PAK-PBD beads. Total lysates before precipitation were probed with actin as the loading control. Statistics were performed using the Student's *t* test, and the p-value is shown in B and E. Error bars show mean + SD. Representative data from two independent experiments is shown in all panels.

igβ- and *igγ*-deficient ticks when compared with the controls (Fig. 3, D and E; and Table S1). PAK1 has been implicated in the rearrangement of the actin cytoskeleton by acting downstream of the small GTPases Rac1 and Cdc42. Upon binding to Rac1/Cdc42, PAK1 autophosphorylates, thereby increasing its kinase activity toward exogenous substrates (Papakonstanti and Stournaras, 2002). We assessed whether *A. phagocytophilum* activates these small GTPases by performing a Rac1/Cdc42 activation assay using the p21–binding domain of PAK1 (PBD) that specifically binds to and precipitates the active (GTP) form of Rac1 and Cdc42. No differences were observed between GTP-Rac1 and GTP-Cdc42 precipitates obtained from *A. phagocytophilum*–infected

or uninfected lysates bound to PAK1-PBD agarose beads (Fig. 3 F and Table S1). Each of the GTPases were assessed with specific antibodies, and an input loading control was provided by tick lysates (before precipitation) probed with actin antibody (Fig. 3 F). Our results suggest that *A. phagocytophilum* induces the *Ixodes* G protein–coupled receptor Gβγ subunits to stimulate IPAK1 and IPI3K activation and that the Rac1/Cdc42 GTPases do not induce IPAK1 activity.

A. phagocytophilum infection alters the ratio of G/F–actin in ticks
PAK1 directly phosphorylates actin, resulting in the disassembly of stress fibers, cortical actin organization, and formation

of filopodia (Papakonstanti and Stournaras, 2002). Moreover, phosphorylation of actin inhibits actin filament nucleation and elongation, leading to a reduction in actin polymerization (Liu et al., 2006). We determined the ratio of globular G (monomeric) to filamentous F (G/F) actin in *A. phagocytophilum*–infected tick cells to examine whether *A. phagocytophilum*–induced actin phosphorylation inhibits actin nucleation and thereby causes alterations in the G/F-actin ratio. *A. phagocytophilum* infection in tick cells increased G-actin and markedly reduced F-actin (threefold; Table S1) in comparison with the uninfected controls (Fig. 4 A and Table S1). In addition, infection with *A. phagocytophilum* also altered the ratio of G/F-actin in unfed nymphal ticks in vivo (unpublished data). Detailed imaging of tick cells using confocal microscopy revealed that filamentous actin-enriched stress fibers/actin bundles were dramatically reduced in the cytosol of *A. phagocytophilum*–infected cells compared with the uninfected controls (Fig. 4 B). In addition, filopodial structures that protrude outside the cell periphery were diminished, with a concomitant increase in G actin staining in cell nuclei of *A. phagocytophilum*–infected cells (Fig. 4 B). When these changes in morphology were quantified, the number of filamentous cells per field, the number of filaments per cell, and the percentage of cells positive for filaments per field were significantly decreased in *A. phagocytophilum*–infected cells in comparison with the uninfected controls (Fig. 4, C–E). Decreased F-actin suggested inhibition of actin polymerization, and increased G-actin in infected cells correlated with the induction of actin phosphorylation by *A. phagocytophilum*.

A. phagocytophilum–induced phosphorylated actin accumulates in cell nuclei and selectively alters *I. scapularis* gene transcription

We assessed whether G-actin was increased in nuclear extracts of *A. phagocytophilum*–infected cells and found increased levels of nuclear actin in comparison with the uninfected controls (Fig. 5 A and Table S1). Confocal microscopy also confirmed higher levels of G-actin in the nuclei of *A. phagocytophilum*–infected cells (Fig. 5 B). Immunoprecipitation with phosphotyrosine antibody showed increased levels of phosphorylated actin in *A. phagocytophilum*–infected nuclear extracts when compared with the uninfected controls (Fig. 5 A and Table S1). To identify a mechanism for *A. phagocytophilum* infection–mediated transcriptional effects, we quantified levels of RNA polymerase II (RNAPII) and the transcription factor TATA box–binding protein (TBP) in uninfected and *A. phagocytophilum*–infected tick cells. Although the total levels of the proteins were not significantly different as a result of infection, immunoprecipitation with RNAPII antibody showed enhanced RNAPII association with TBP, suggesting that a stable interaction of TBP and RNAPII is induced upon infection with *A. phagocytophilum* (Fig. 5 A and Table S1).

Actin has been shown to associate with eukaryotic RNA polymerases and is directly involved in gene transcription (Bettinger, et al., 2004; Hofmann, 2009). We noted an increased association of G-actin or phosphorylated actin with RNAPII in *A. phagocytophilum*–infected tick cell nuclei in comparison with the uninfected controls (Fig. 5, C and D). These data suggest a role for *A. phagocytophilum*–induced
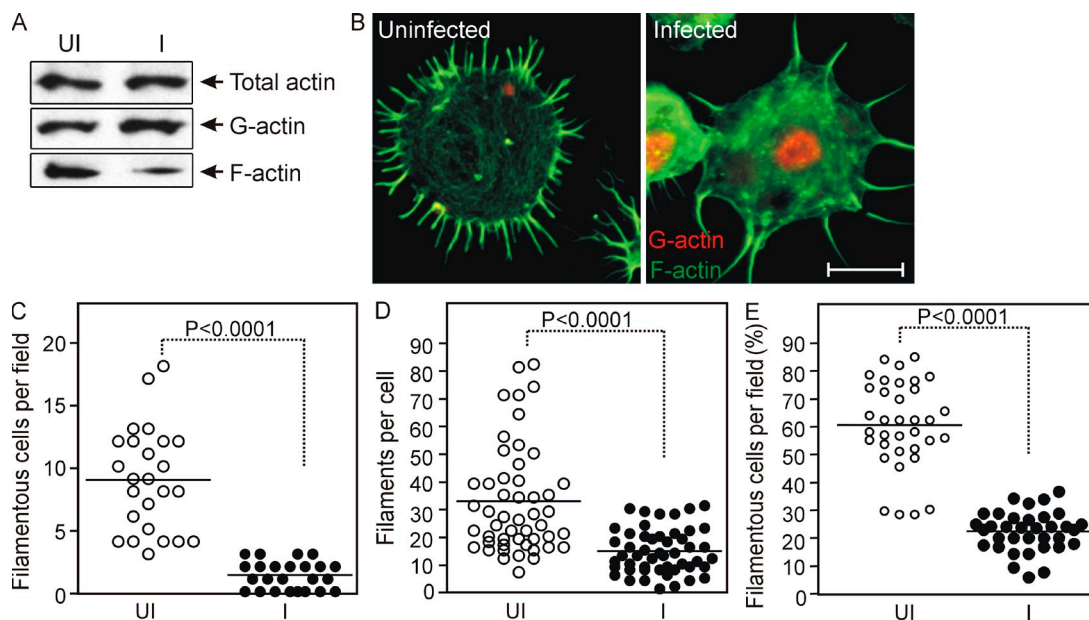

Figure 4. *A. phagocytophilum* infection alters the G/F–actin ratio in tick cells. (A) Immunoblots of F-actin and G-actin in *A. phagocytophilum*–infected tick cells (I) in comparison with the uninfected controls (UI). Total lysate used for separation of G/F actin (supernatant/pellet) ratio was probed with anti-actin as the loading control. (B) Immunofluorescence images of uninfected and *A. phagocytophilum*–infected tick cells stained for F-actin (green) and G-actin (red). Bar, 10 µm. (C) Quantification of the number of filamentous cells per microscopic field, using 25 random fields, is shown. (D) The number of filaments per cell, examining 50 cells in each group, is shown. (E) The percentage of cells positive for F-actin filaments was quantified from 35 random microscopic fields. Statistics were performed using the Student's *t* test and the p-value is shown. Three independent experiments yielded similar results.
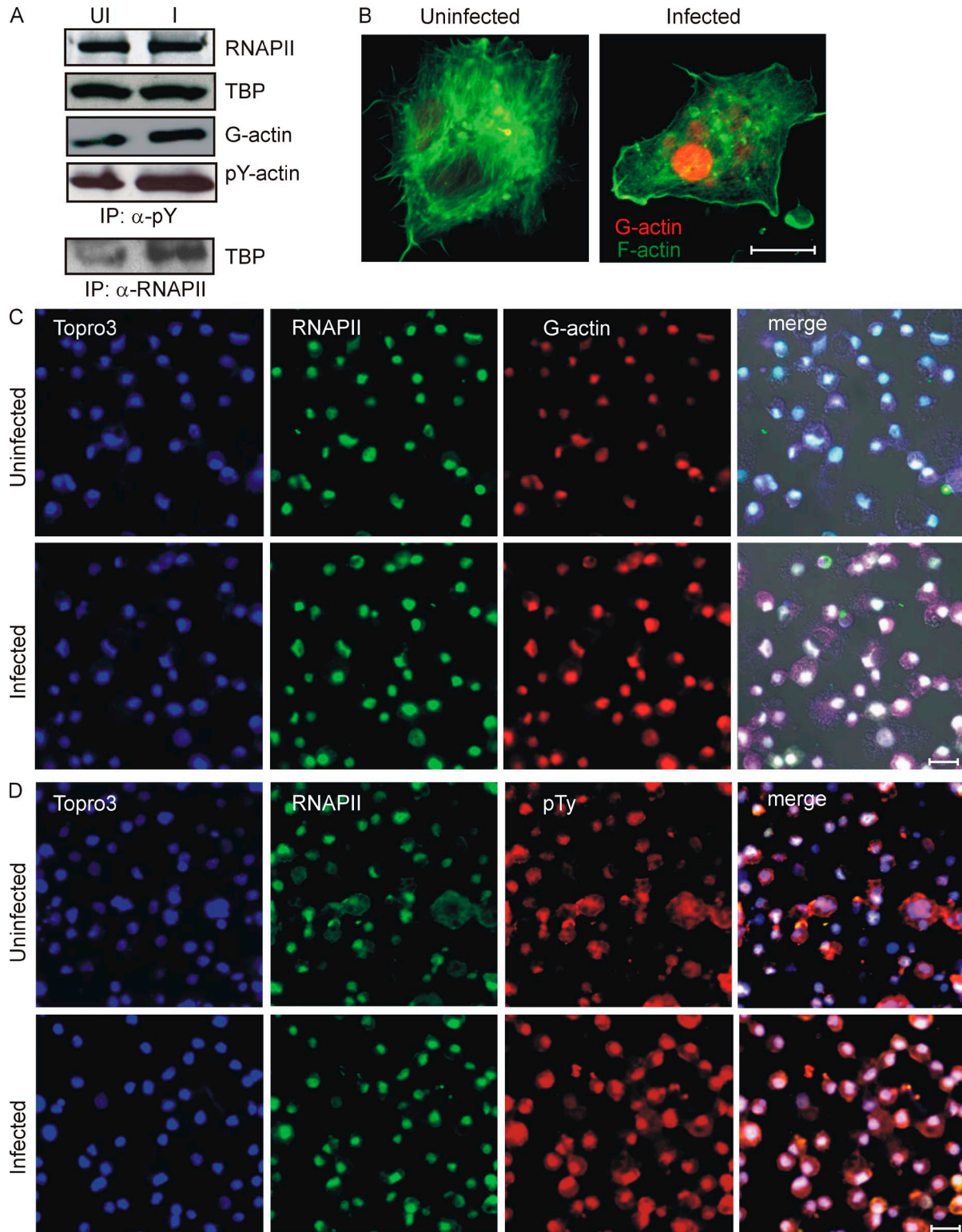
Figure 5. *A. phagocytophilum*–induced phosphorylated/G–actin accumulates in tick cell nuclei. (A) Nuclear extracts were prepared from uninfected (UI) and *A. phagocytophilum*–infected (I) cells and subjected to immunoprecipitation (IP) and immunoblot (IB) with the indicated antibodies. Immunoblots for RNAPII and TBP served as loading control. Three independent experiments yielded similar results. (B) Confocal microscopy showing G-actin (red) and F-actin (green) in *A. phagocytophilum*–infected (I) or uninfected (UI) tick cells. Bar, 10 µM. (C and D) Uninfected and infected tick cells were stained with DNase I for G-actin (red; C) or anti-phosphotyrosine (red; D) and anti RNAPII (green) and TOPRO-3 (blue). Representative images from three independent experiments are shown. Bars, 20 µm.
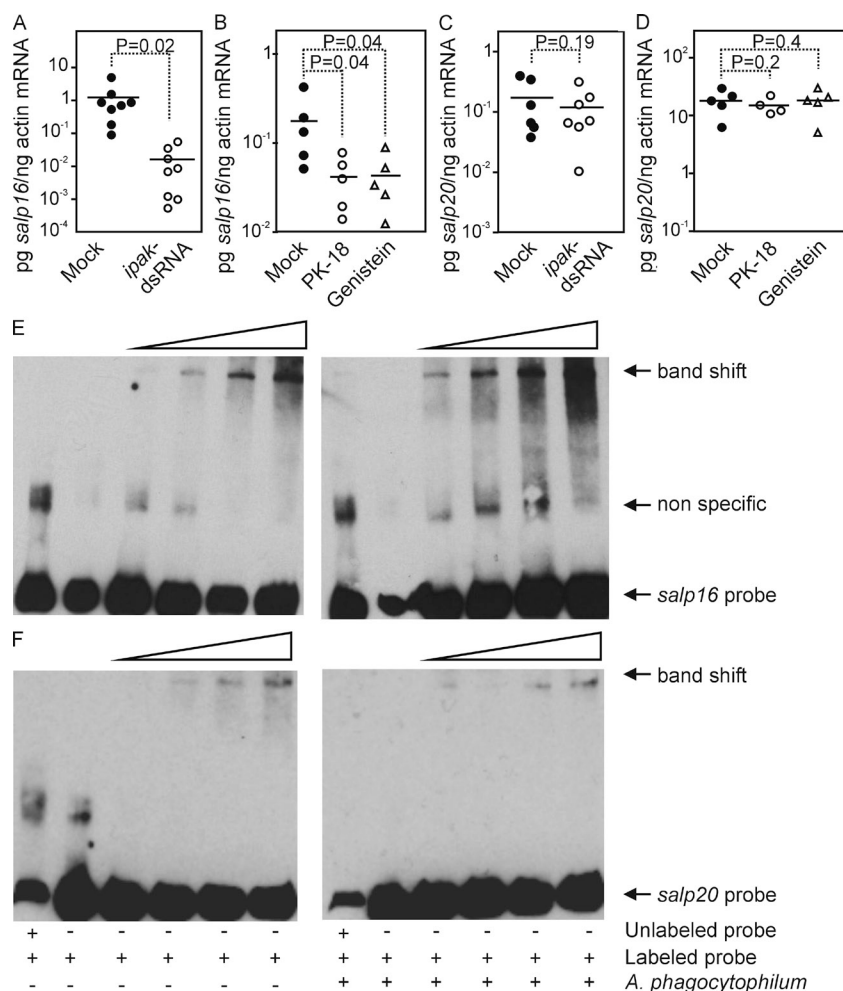
Figure 6. *A. phagocytophilum*–induced actin phosphorylation selectively regulates *I. scapularis salp16* gene expression. Q-RT-PCR results showing the levels of *salp16* or *salp20* in *ipak1*-dsRNA– (A and C), PK-18– (PAK1 inhibitor), or Genistein (tyrosine kinase inhibitor)-injected ticks, respectively (B and D). Mock controls were injected with buffer alone (A and C) or DMSO (B and D), respectively. The levels of *salp16* or *salp20* transcripts were quantified against tick *β-actin* transcripts. Each circle represents an individual tick. Statistics were performed using a Student's *t* test and the p-value is shown. Horizontal bars in A–D indicate mean values of the data points. (E and F) EMSAs performed with the biotin-labeled *salp16* (E) or *salp20* (F) promoter TATA-binding regions and uninfected or *A. phagocytophilum*–infected nuclear extract proteins. Shifts and the *salp16*- or *salp20*-free probes are indicated with arrows. Representative gel images from three independent experiments are shown. Wedges indicate increasing amounts of nuclear extracts (1, 1.5, 2, and 2.5 µg).

putative *salp16* promoter TATA binding motif in comparison with the nuclear extract proteins from uninfected controls (Fig. 6 E). EMSAs with the *salp20* probe showed no differences in binding for nuclear extract proteins from *A. phagocytophilum*–infected or uninfected nuclear extract proteins (Fig. 6 F). These data were consistent with the quantitative (Q) RT-PCR showing no alterations in *salp20* gene expression in *ipak1*-silenced or inhibitor-treated *A. phagocytophilum*–infected ticks (Fig. 6, C and D). EMSA performed with tick nuclear extract proteins from *A. phagocytophilum*–infected ticks and antibodies against RNAPII, TBP, phosphotyrosine, or actin blocked the band shift with *salp16* probe (Fig. S7 A), suggesting an important role for these nuclear proteins in regulating *salp16* gene transcription. EMSAs with actin antibody (increasing concentrations) and nuclear extracts from *A. phagocytophilum*–infected ticks showed a band shift with the *salp20* probe. However, the band shift was reduced or blocked with the *salp16* probe, suggesting a specific role for phosphorylated nuclear actin in selective regulation of *salp16* gene transcription (Fig. S7 B).

In addition to *salp16* and *salp20* genes, we analyzed several other *salp* genes such as *salp15* (Fig. 7, A and B), *salp17* (Fig. 7, C and D), and *salp25D* (Fig. 7, E and F). Upon *ipak1*-silencing or treatment with inhibitors (PK-18 or Genistein), we found no significant difference in the expression levels of these genes. Furthermore, no alterations were seen in *β-tubulin* or *gapdh* expression levels upon either *ipak1*-silencing or treatment with inhibitors (PK-18 or Genistein; Fig. 7, G–J). Although not exhaustive, the unchanged transcription levels of this panel of genes suggest that IPAK1-mediated actin phosphorylation is not a global regulator but rather has a selective effect on *salp16* after *A. phagocytophilum* infection. Collectively, our data suggest a novel role for *A. phagocytophilum*-induced phosphorylated actin

phosphorylated actin in altering gene transcription. To address the role of phosphorylated actin in modulating *Ixodes* gene transcription, we examined an *A. phagocytophilum*–modulated tick gene, *salp16*, which we have shown to be essential for *A. phagocytophilum* survival in ticks (Sukumaran et al., 2006). During *A. phagocytophilum* acquisition by the tick, *salp16* expression levels were elevated in mock-injected ticks, as expected, but were significantly reduced in both *ipak1*-silenced and PAK1 inhibitor–injected ticks (Fig. 6, A and B). Silenced *ipak1* levels and reduced actin phosphorylation correlated with significantly decreased *salp16* levels in *A. phagocytophilum*-infected ticks. To assess whether the reduction in *salp16* gene expression was specific in *ipak1*-silenced or PAK1 inhibitor–treated *A. phagocytophilum*–infected ticks, we analyzed the expression levels of *salp20* gene from *I. scapularis*. We found no significant alterations in the expression levels of *salp20* (Fig. 6, C and D).

To establish a possible mechanism for the specific enhancement of expression of *salp16* in *A. phagocytophilum*–infected ticks, we identified a putative RNAPII-dependent promoter TATA motif in the genomic locus of *salp16* and *salp20* (as control), as indicated in the experimental procedures. Electrophoretic mobility shift assays (EMSAs) showed enhanced binding of crude nuclear extracts from *A. phagocytophilum*–infected ticks to the
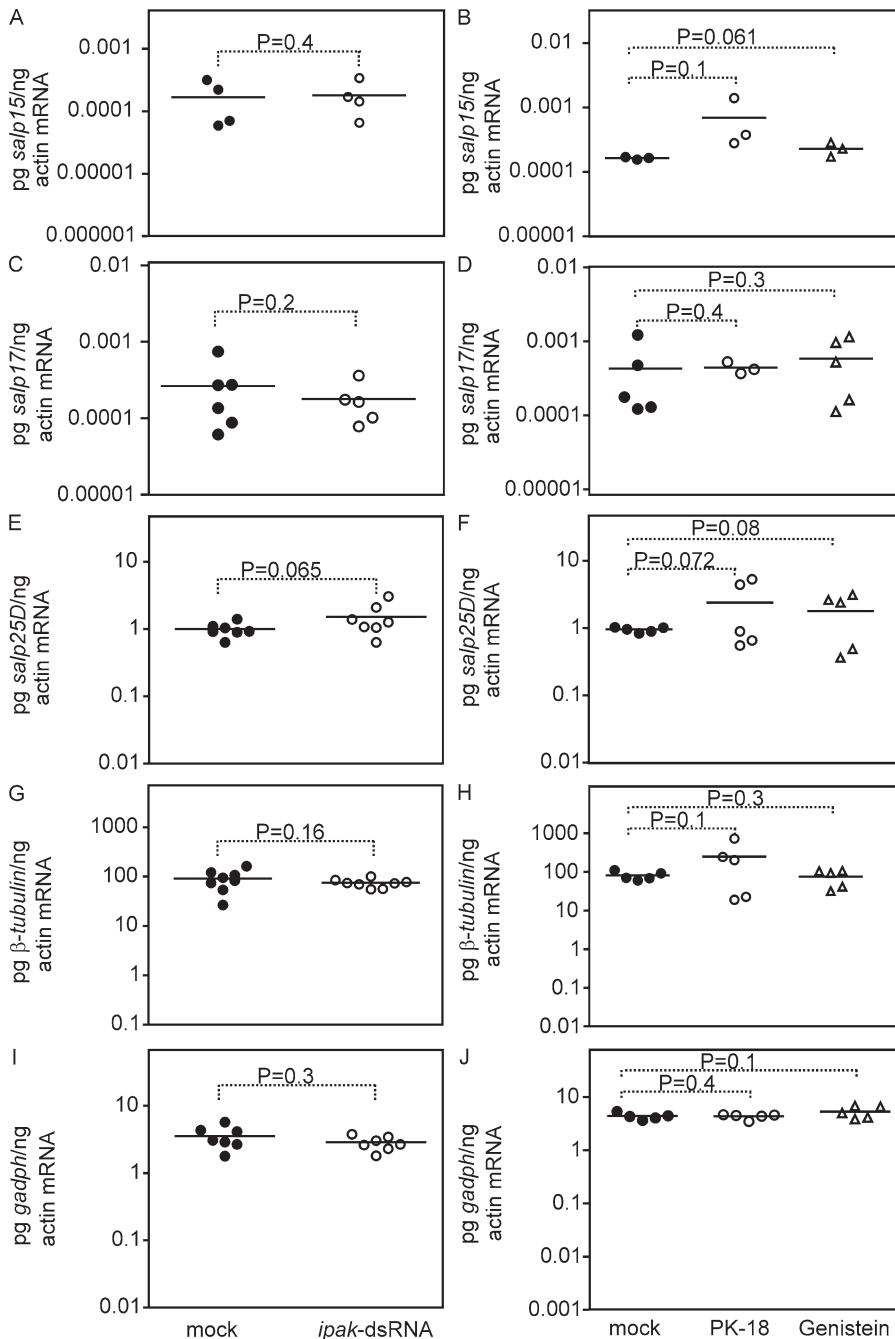
Figure 7. Silencing or Inhibition of *ipak1* does not alter *salp15*, *salp17*, *salp25D*, *β-tubulin*, or *gapdh* gene expression. Q-RT-PCR showing levels of *salp15* (A and B), *salp17* (C and D), *salp25D* (E and F), *β-tubulin* (G and H), and *gapdh* (I and J) mRNA in mock and *ipak1*-dsRNA–injected ticks (A, C, E, G, and I) and in mock or PK-18– (PAK1 inhibitor) or Genistein (tyrosine kinase inhibitor)–injected ticks (B, D, F, H, and J). Mock controls were injected with buffer alone (A, C, E, G, and I) or DMSO (B, D, F, H, and J), respectively. The levels of transcripts were quantified against tick *β-actin* transcripts. Each circle represents an individual tick. Statistics were performed using the Student's *t* test, and the p-value is shown. Horizontal bars in all panels represent mean values of the data points.

levels were dramatically reduced in nuclear extracts from *ipak1*-silenced ticks as compared with the mock (buffer alone) control (Fig. 8 A and Table S1). The levels of TBP and RNAPII were unaffected in nuclear extracts from both mock and *ipak1*-silenced samples (Fig. 8 A and Table S1). Total actin levels from the same lysates served as loading control (Fig. 8 A). EMSAs with a *salp16* probe showed reduced binding with nuclear extract proteins from *ipak1*-silenced ticks, further demonstrating the importance of IPAK1-mediated actin phosphorylation in selective regulation of *salp16* gene transcription (Fig. 8 B). No differences were observed in the band shifts with the *salp20* probe (Fig. 8 B). The combined data from Fig. 8 (A and B) suggest that lower levels of phosphorylated actin in the nuclear extracts from *ipak1*-silenced ticks specifically affects *salp16* but not *salp20* gene transcription. To directly show that IPAK1-mediated actin phosphory-

in association with RNAPII and TBP as important components of the transcriptional activation required to selectively regulate *I. scapularis salp16* gene transcription.

A. phagocytophilum–induced phosphorylated actin mediates promoter specificity for selective regulation of *salp16* gene transcription

To confirm that IPAK1-mediated phosphorylated actin is responsible for the selective regulation of *salp16* transcription upon *A. phagocytophilum* infection, we analyzed the levels of phosphorylated actin, TBP, and RNAPII in mock and *ipak1*-silenced nuclear extracts from ticks. The phosphorylated actin

lation plays a novel role in selective regulation of *salp16* gene transcription, we performed a DNA affinity precipitation (DNAP) assay using nuclear extracts from *A. phagocytophilum*–infected ticks and *salp16* or *salp20* promoter regions. The DNAP assay showed that phosphorylated actin binding was enhanced and specific to the *salp16* probe (Fig. 8 C and Table S1). No differences were observed for either TBP or RNAPII binding to the *salp16* or *salp20* probes (Fig. 8 C and Table S1), further strengthening the conclusion that a potential novel role for *A. phagocytophilum*–induced phosphorylated actin in the nucleus is selective regulation of *salp16* promoter. The nuclear lysates from *A. phagocytophilum*–infected ticks used
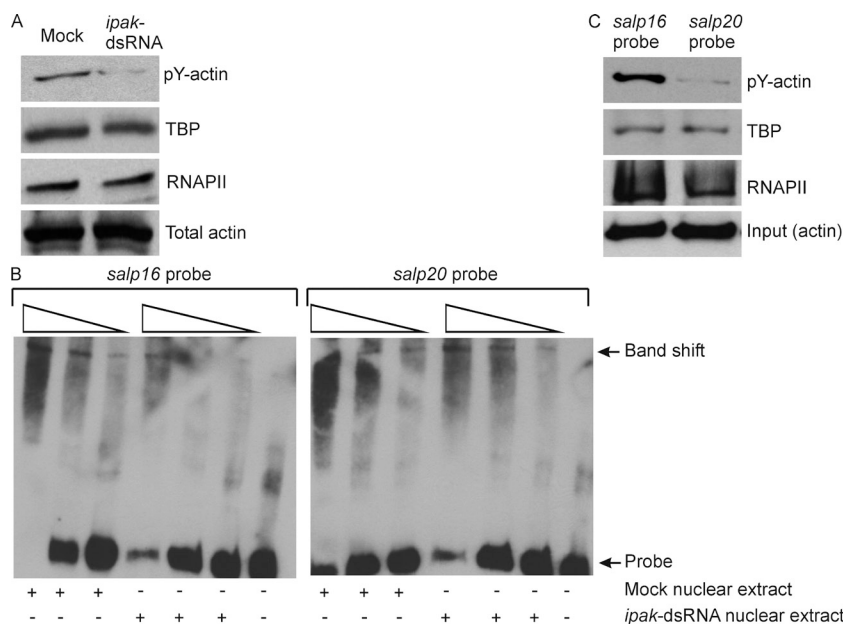
Figure 8. *A. phagocytophilum*–induced actin phosphorylation selectively mediates *I. scapularis salp16* gene promoter specificity. (A) Immunoblots showing the levels of phosphorylated actin, TBP, and RNAPII in *A. phagocytophilum*–infected mock (buffer alone) or *ipak1*-silenced tick nuclear extracts. Total actin served as the loading control. (B) EMSAs performed with the biotin-labeled *salp16* or *salp20* promoter TATA-binding regions and *A. phagocytophilum*–infected mock or *ipak1*-silenced nuclear extract proteins. Band shifts, *salp16*-, or *salp20*-free probes are indicated with arrows. Wedges indicate decreasing amounts of nuclear extracts (3, 2, and 1 μg). (C) Biotinylated DNAP with *salp16* or *salp20* probes and *A. phagocytophilum*–infected nuclear extract proteins. DNA precipitates were probed with actin-pTyr, anti-TBP, or anti-RNAP. Nuclear extracts were probed with anti-actin (input) as a loading control. Representative gel images from three independent experiments are shown in all panels.

for the DNAP assay were probed with actin antibody as the loading control (Fig. 8 C). Collectively, the results from mock/*ipak1*-silenced tick nuclear extracts (Fig. 8, A and B), EMSAs performed with actin antibody blocking (Fig. S7 B), and the DNAP assay (Fig. 8 C) show that *salp16* promoter specificity is mediated by phosphorylated actin to selectively regulate *Ixodes* gene transcription.

DISCUSSION

Obligate intracellular bacteria have evolved a variety of mechanisms to persist in their hosts, including modulating host signaling and the actin cytoskeleton (Bhavsar et al., 2007). We addressed the survival strategies that *A. phagocytophilum* uses to persist in its arthropod vector *I. scapularis*. We provide in vitro and in vivo evidence that *A. phagocytophilum* induces the phosphorylation of actin and alters the ratio of monomeric/filamentous (G/F) actin leading to translocation of phosphorylated/G-actin into the cell nucleus. *A. phagocytophilum*-induced actin phosphorylation was dependent on Gβγ stimulation involving the activation of *Ixodes* PI3K and PAK1 but was independent of Rac1/Cdc42 small GTPases. The ability of the bacteria to enhance levels of phosphorylated actin in the nucleus selectively regulates *I. scapularis salp16* gene transcription in association with RNAPII and TBP. This is the first study demonstrating that an intracellular bacterium can exploit phosphorylated actin to specifically control gene transcription in its arthropod host.

Generally, a small percentage of the total pool of a certain protein is phosphorylated in cells and this transient change is sufficient to activate signaling (Pawson and Scott, 2005). *A. phagocytophilum*-induced actin phosphorylation was maintained stably for several days (in vitro) to months (in vivo) suggesting that it is an extended modification. Phosphorylation and dephosphorylation of proteins is executed by pro-

tein kinases and phosphatases (Pawson and Scott, 2005). Studies with pervanadate indicated that *A. phagocytophilum* does not inhibit the host phosphatase activity to induce actin phosphorylation. The stable modification of actin also occurred in unfed *A. phagocytophilum*–infected ticks and when clean ticks were fed on *A. phagocytophilum*–infected mice. Recently, our group has shown that *A. phagocytophilum* influences cell signaling, specifically the tyrosine phosphorylation of ROCK1, to facilitate infection in human neutrophils (Thomas and Fikrig, 2007). Actin phosphorylation was not induced in *A. phagocytophilum*–infected primary cultures of human neutrophils (Fig. S7 C), suggesting that this stable modification occurs specifically in the arthropod vector.

Heterotrimeric G proteins have been implicated in PAK1 and PI3K activation (Menard and Mattingly, 2004). Previous studies have also shown that the association of PI3K with PAK1 phosphorylates actin and reorganizes the actin cytoskeleton (Papakonstanti and Stournaras, 2002). PAK1 also directly phosphorylates actin, resulting in the disassembly of stress fibers, cortical actin organization, and cytoskeletal remodeling (Sells et al., 1997, 1999; Papakonstanti and Stournaras, 2002). It was noteworthy that *A. phagocytophilum*–induced actin phosphorylation was associated with the increase in the amount of actin that interacts with IPAK1. Furthermore, the increased levels of *Ixodes gβ*, *gγ*, *ipi3k*, and *ipak1* in *A. phagocytophilum*–infected ticks and clean ticks acquiring *A. phagocytophilum* from mice, as well as the enhanced association of IPAK1 and actin in tick cells, suggest that actin phosphorylation in *I. scapularis* results from PI3K- and PAK1-mediated signaling. *A. phagocytophilum*–induced IPAK1 activation and increased actin phosphorylation was dependent on Gβγ stimulation involving PI3K activation but was independent of Rac1/Cdc42 small GTPases. The ability of PI3K and IPAK1 to markedly inhibit both *A. phagocytophilum*–induced actin phosphorylation

and bacterial survival in tick cells, infected ticks, and ticks that acquire bacteria from the mouse host demonstrates that PI3K-PAK1 signaling plays an important role in these events. The *Ixodes gβ–*, *gγ–*, *pi3k–*, and *pak1*-deficient ticks also showed a marked reduction in the levels of phosphorylated actin and the *A. phagocytophilum* burden. Collectively, these data show that *Ixodes* PI3K-PAK1–mediated signaling and IPAK1-actin association facilitates *A. phagocytophilum* survival in the vector.

In eukaryotic cells, actin exists in two forms: globular (G) monomeric actin and filamentous (F) polymerized actin. G-actin with bound ATP can polymerize to form F-actin, which hydrolyzes bound ATP releasing ADP and P_i to form G-actin–ADP monomers (Gerisch et al., 1991; Pollard and Borisy, 2003). Actin is a common target of many bacterial proteins, and the cellular responses induced by a variety of stimuli and pathogens involve changes in cell morphology and the polymerization state of actin (Cameron et al., 2000; Gouin et al., 2005; Stevens et al., 2006). Our study demonstrated that *A. phagocytophilum* is unique among intracellular bacterial pathogens in altering G/F-actin levels to inhibit the actin polymerization machinery in the arthropod vector. The increased G-actin and reduced F-actin levels in *A. phagocytophilum*–infected tick cells suggest that *A. phagocytophilum* may inhibit actin filament nucleation and elongation by inducing actin phosphorylation. Our data complement the previous finding that phosphorylation of actin substantially inhibits nucleation and rate of polymerization of actin filaments in *Dictyostelium* (Jungbluth et al., 1994; Liu et al., 2006). Phosphorylation of actin was also associated with rearrangements of the actin cytoskeleton where filamentous actin-enriched stress fibers/actin bundles in the cytosol and filopodial structures protruding outside the cell periphery were dramatically reduced in *A. phagocytophilum*–infected cells. PAK1-mediated phosphorylation of actin and their direct association also results in the disassembly of actin stress fibers and cortical actin organization (Papakonstanti and Stournaras, 2002), further supporting the correlation between *A. phagocytophilum*–induced PAK1-mediated actin phosphorylation and the remodulation of the actin cytoskeleton in the arthropod vector. Overall, these findings detail a mechanism of host cytoskeletal subversion by *A. phagocytophilum* to alter actin nucleation in its arthropod vector.

Several studies have demonstrated the presence of actin in the nucleus and that nuclear actin is essential for transcription by RNA polymerases, transcription regulation, RNA processing and export, chromatin remodeling, intranuclear movement, and structure maintenance (Pederson and Aebi, 2002; Bettinger et al., 2004; Hofmann et al., 2004; Percipalle and Visa, 2006; Hofmann, 2009). Actin may exist in monomeric form (Hofmann and de Lanerolle, 2006; Hofmann, 2009) or as short polymers of less than seven monomers in the nucleus that differ from cytosolic filamentous actin (Hofmann and de Lanerolle, 2006; Hofmann, 2009). Our results show that *A. phagocytophilum*–induced phosphorylation of actin leads to increased monomeric (G) actin levels that predominantly localize to the cell nucleus (Figs. 4 and 5). G-actin staining and phosphorylation signals were also dramatically enhanced in the

nucleus of *A. phagocytophilum*–infected cells and showed a strong association with RNAPII. Actin binds RNA polymerase I, II, and III and is required for the formation of preinitiation complexes (Pederson and Aebi, 2002; Bettinger et al., 2004; Hofmann et al., 2004; Percipalle and Visa, 2006; Hofmann, 2009). The enhanced G-actin levels in *A. phagocytophilum*–infected cell nuclei and its association with RNAPII suggested a role for actin phosphorylation in mediating host gene transcription. It has previously been shown that *A. phagocytophilum* induces tick *salp16* gene expression and that Salp16 is essential for the survival of this microbe in ticks (Sukumaran et al., 2006). The reduction in actin phosphorylation in *ipak1*-deficient ticks correlated with a decrease in *salp16* gene expression. Using the *salp20* gene (which is not differentially expressed upon *A. phagocytophilum* infection) promoter fragment as control, we have analyzed the reason for the selective regulation of *salp16* gene. Our results with *ipak1*-silenced tick nuclear extracts (which contain less phosphorylated actin), EMSAs with actin antibody, and DNAP showed that specificity for the *salp16* promoter is mediated by the enhanced accumulation of phosphorylated actin that leads to the greater stability of RNAPII and TBP complex formation. These results lead us to propose a model wherein *A. phagocytophilum*–induced actin phosphorylation is followed by the inhibition of actin nucleation and rate of actin polymerization, therefore resulting in decreased F-actin and increased G-actin levels in the cell (Fig. S8). The increased G-actin (phosphorylated actin) levels are recruited to the nucleus to enable the formation of stable preinitiation complexes and selective regulation of *Ixodes* gene transcription. The stable preinitiation complexes formed with phosphorylated actin may enable tight binding and the enhanced interaction of RNAPII to TBP, which may eventually lead to selectively increased RNAPII dependent *salp16* gene expression during *A. phagocytophilum* infection.

The fundamental mechanism by which arthropod gene regulation is manipulated by pathogens is not understood. Our results provide valuable insight into understanding how a microbe can exploit actin to selectively control arthropod gene expression to beneficially survive in the vector. This knowledge will be useful in the development of methods to interrupt the *A. phagocytophilum*–tick cycle, which may ultimately lead to the prevention of this *I. scapularis*–borne illness. We are also hopeful that these findings will be useful in developing new strategies, based on targeting pathogen–vector interactions, to combat many other arthropod-borne diseases of medical importance.

MATERIALS AND METHODS

A. phagocytophilum infection, cell lines, and culture conditions. Human promyelocytic cell line (HL-60) was acquired from American Type Culture Collection and maintained at 37°C in 5% CO_2 in IMDM (Invitrogen) with 20% FCS. *A. phagocytophilum* infection was analyzed by immunofluorescence, and cell-free bacteria were collected from ∼95% *A. phagocytophilum*–infected HL-60 cells by centrifugation for 10 min at 4,000 rpm. Cell pellets were resuspend in IMDM, lysed by six passages through a 25-guage, followed by six more passages through a 27-guage needles, and the lysates were centrifuged at 1,200 rpm for 3 min to obtain cell-free bacteria in the supernatants. Bacteria were used to infect *I. ricinus* tick cell line IRE/CTVM19 (Bell-Sakyi et al., 2007), maintained at 28°C without CO_2 as previously described (Pedra et al., 2010).

***I. scapularis* ticks and mice.** *I. scapularis* uninfected and *A. phagocytophilum*–infected nymphal ticks (L. Rollend, c/o Dr. Durland Fish laboratory, Department of Epidemiology and Public Health, Yale University, New Haven, CT) were obtained from a continuously maintained tick colony at the Department of Epidemiology and Public Health at Yale University (New Haven, CT). Because *A. phagocytophilum* is transstadially transmitted, we produced *A. phagocytophilum*–infected nymphs by feeding uninfected larvae to repletion on *A. phagocytophilum*–infected C3H/HeN mice and subsequently allowing them to molt into nymphs, a process which takes several months in tick metamorphosis. *A. phagocytophilum* infection rates in nymphs were individually tested by PCR to confirm infection and were determined to be 82 ± 13% from each infection group. The uninfected control nymphs were produced by feeding larvae on uninfected mice and then allowing them to molt. Tick rearing and molting was conducted in an incubator at 23°C with 85% relative humidity and a 14/10-h light/dark photo period regiment. All tick feeding experimental protocols followed Yale University institutional guidelines for care and use of laboratory animals and were approved by the Institutional Animal Care and Use Committee at Yale University.

***A. phagocytophilum* acquisition studies.** The *A. phagocytophilum* isolate NCH-1 (which also infects humans) was maintained through serial passages of infected blood in C3H/SCID mice (The Jackson Laboratory). For the acquisition experiments, C3H/HeN immunocompetent mice (Charles River Laboratories) were injected intraperitoneally with 100 µl of *A. phagocytophilum*–infected or uninfected (controls) anticoagulated blood pooled from C3H/SCID mice. Q-PCR was performed on an aliquot of the pooled blood collected from the SCID mice to determine *A. phagocytophilum* infection. For acquisition experiments, uninfected ticks were fed on either *A. phagocytophilum*–infected or naive C3H/HeN mice (3 mice per group and 20 ticks per mice were used in all the acquisition/feeding studies). The bacterial loads in the mouse peripheral blood were assessed by Q-PCR on day 6 (Sukumaran et al., 2006) and ticks were allowed to feed on day 7 after infection (the interval of maximum *A. phagocytophilum* infection in mice). Ticks were collected at 24, 48, and 72 h during feeding and 48 and 72 h after repletion. We repeated all the feeding experiments to rule out any bias on *A. phagocytophilum* acquisition by the tick as a result of mouse-to-mouse or tick–tick variations in the bacterial load and obtained identical results with the independent batches.

Immunoprecipitation. Tick cell lysates were prepared from uninfected and *A. phagocytophilum*–infected cells (48 h after infection). Cell pellets (10^7 cells /ml) were washed twice with PBS and resuspended in cold modified RIPA buffer containing protease (Roche) and phosphatase (Sigma-Aldrich) inhibitors. The lysates were precleared with protein A/G agarose beads (Thermo Fisher Scientific) at a 1:10 volume of 50% bead slurry and centrifuged at 12,000 rpm at 4°C for 10 min. The supernatants were collected and protein concentrations were determined using the Bradford assay (BCA kit; Thermo Fisher Scientific). For analyzing the phosphorylation of proteins upon *A. phagocytophilum* infection in tick cells, antibodies specific to phosphotyrosine (Cell Signaling Technologies) were added to 500 µg/ml of the lysate and the mixture was incubated overnight at 4°C. Immunoprecipitates were also processed for Western blotting with actin antibody (Millipore) to further confirm actin phosphorylation. For determining the interaction between *Ixodes* PAK1 and actin, 500 µg of uninfected or *A. phagocytophilum*–infected lysates were immunoprecipitated with PAK1 antibody (Cell Signaling Technologies), followed by immunoblotting with actin antibody (Cytoskeleton, Inc.). For immunoprecipitations using nuclear extracts, 200–400 µg of the tick lysate were incubated with either phosphotyrosine or RNAPII (Abcam) antibodies, respectively. After incubation with the respective antibodies, protein A/G beads were added and the mixture was incubated for an additional 4 h to overnight at 4°C. Beads were pulse collected by cold centrifugation, washed three times with cold PBS, resuspended in SDS sample buffer, boiled for 5 min, and supernatants were run on 12% SDS-PAGE gels (Bio-Rad Laboratories). Gels were either transferred to nitrocellulose membranes for immunoblotting or stained with Coomassie blue to analyze induction in protein phosphorylation or changes in total protein profile.

Immunofluorescence and confocal microscopy. Uninfected and *A. phagocytophilum*–infected tick cells were fixed with 3.7% (wt/vol) paraformaldehyde (37°C for 20 min), permeabilized with 0.2% (vol/vol) Triton X-100 (10 min at room temperature), and blocked with 3% bovine serum albumin (30 min at room temperature) in PBS, respectively. Cells were immunostained with antibodies directed against phosphotyrosine, actin, or RNAPII, and labeling was detected by anti–mouse secondary antibodies conjugated with Alexa Fluor 488 or 594, respectively. *A. phagocytophilum* was detected using polyclonal antiserum as previously described (Pedra et al., 2010). Cells were incubated with either 1 µg/ml phalloidin–Alexa Fluor 488 or with DNase I–Alexa Fluor 594 conjugates to stain for F- or G-actin, respectively. To quantify number of filamentous cell per field, a minimum of 25 microscopic fields were considered and the number of filamentous cells was counted from each field. To determine the number of filaments per cell, the total number of F-actin–positive filaments on the cell periphery that strongly stained with phalloidin was counted from a total of 50 cells in each group. The percentage of cells positive for filaments was determined by counting the number of filamentous cells/field to the total number of cells in that field. Three independent experiments were performed to determine statistical significance. Confocal images of G/F-actin were captured simultaneously at similar intensities and relevant excitation and emissions, respectively. Cells were counterstained for nuclei with TOPRO3–Alexa Fluor 647 conjugate. For tick salivary glands, immunofluorescence was performed as previously described (Sukumaran et al., 2006; Neelakanta et al., 2007). Salivary glands were dissected from unfed ticks, fixed with ice-cold acetone, and washed in PBS. Microscope slides containing fixed permeabilized tissue sections were blocked with PBS containing 0.05% Tween 20 and 5% goat serum for 1 h at 37°C and were sequentially incubated with actin and phosphotyrosine antibodies, followed by anti–mouse secondary antibodies conjugated with Alexa Fluor 488 or 594, respectively. All Alexa conjugates were obtained from Invitrogen. Images were acquired using a laser-scanning confocal microscope (LSM 510; Carl Zeiss, Inc.).

Identification of PI3K and PAK1 from the *Ixodes scapularis* genome. The *I. scapularis* genome database VectorBase (http://iscapularis.vectorbase.org/index.php) includes all genomic data (e.g., EST sequences, trace files, scaffolds, assemblies, and automated annotations) and the database at The Gene Index Project database includes EST sequences. The *ipak1* and *ipi3k* partial nucleotide sequences were identified with the BLAST search performed at The Gene Index Project in the *I. scapularis* EST database. EST sequences corresponding to *I. scapularis ipak1* (Gene Index Project accession no. TC39943) and *ipi3k* (Gene Index Project accession no. TC38262) were identified with a BLAST search using *Drosophila melanogaster pak1* (NCBI nucleotide accession no. DMU56080) and *pi3k* (accession no. NM_057785) nucleotide sequences as queries, respectively. EST sequences were further analyzed using DNASTAR software. Total RNA from unfed uninfected *I. scapularis* ticks was processed for cDNA synthesis and used as template for RT-PCR. The *ipak1* fragment was amplified using oligonucleotides 5′-ATGGCTCAGCTACGGGCCGT-3′ and 5′-TTAGACCTTGTTCAGCACCTTCTTG-3′ and *ipi3k* fragment was amplified using 5′-GCTCTTCAAGTCCGCCCTCA-3′ and 5′-GGACAAACCCGTGCTTCGT-3′. The generated PCR products were cloned into pGEM-T easy vector (Promega) and sequenced using primers 5′-CGCCAGGGTTTTCCCAGTCACGAC-3′ and 5′-CACACAGGAAACAGCTATGAC-3′ from both the ends (KECK Sequencing Facility, Yale University). Amino acid sequence similarity and identity of *Ixodes* PAK1 and PI3K was determined by aligning deduced amino acid sequences with human, mouse, mosquito, and *Drosophila* PAK1 and PI3K using DNASTAR software.

Measurement of G/F-actin ratios. The amount of F-actin compared with free G-actin content was determined by G/F-actin in vivo assay kit (Cytoskeleton, Inc.) according to the manufacturer's instructions. In brief, unfed uninfected ticks, *A. phagocytophilum*–infected ticks or tick cells at 48 h after infection, and uninfected tick cells were homogenized in lysis and F-actin stabilization buffer followed by centrifugation for 1 h at 100,000 *g* at 30°C to separate the F-actin from G-actin pool. Supernatants of the protein extracts were collected after centrifugation and stored on ice. Pellets were resuspended in ice-cold

distilled H$_2$O plus 1 µmol/liter cytochalasin D and incubated for 1 h on ice to disassociate F-actin by gently mixing for every 15 min. Equal amounts of both the supernatant (G-actin) and the resuspended pellet (F-actin) were subjected to analysis of immunoblot with the actin antibody (Cytoskeleton, Inc.). Total lysates (input) probed for total actin served as the loading control.

Nuclear extraction and EMSA. Nuclear extracts were prepared from uninfected and *A. phagocytophilum*–infected ticks or mock and *ipak1*-dsRNA–injected ticks (48 h during feeding) using NE-PER Nuclear and Cytoplasmic extraction kit (Thermo Fisher Scientific) according to the manufacturer's instructions. Gel shift assays were performed with the LightShift chemiluminescent EMSA kit (Thermo Fisher Scientific). Complementary biotinylated oligonucleotides consisting of the *salp16* putative promoter TATA binding region 5′-GCCACGCCTAATG-CATTCCCGGTATATAAGAAAGAAAGAAGCCTCCTGGA-3′ and 5′-TCCAGGAGGCTTCTTTCTTTCTTATATACCGGGAATGCAT-TAGGCGTGGC-3′ or *salp20* putative promoter TATA binding region 5′-TTGGTGCTTGCAAGCTCGTGGGTATATATATATATC-GGCGAAGGATTATGACAT-3′ and 5′-ATGTCATAATCCTTCGCC-GATATATATACCCACGAGCTTGCAAGCACCAA-3′ were annealed and biotin labeled according to the Biotin 3′ End DNA labeling kit (Thermo Fisher Scientific). The respective labeled oligonucleotides were added to a 20-µl reaction mix consisting of 1–3 µg of the nuclear extracts, DNA binding buffer, Poly (dI-dC), 1% NP-40, and MgCl$_2$ in concentrations based on the manufacturer's recommendations. For competition assays, unlabeled oligonucleotides were allowed to bind the nuclear extracts (30 min at room temperature) before the addition of labeled probes. EMSAs were performed with antibodies by incubating 1–3 µg of the respective antibodies with nuclear extract proteins (2 µg for 30 min at room temperature). The reactions were incubated for additional 20 min with respective labeled probes, followed by loading onto a 6% native DNA polyacrylamide gel. The gel was prerun and run with 0.5% Tris-Borate-EDTA and processed according to the manufacturer's instructions.

Neutrophil isolation. PBMCs were isolated from a healthy donor with no acute illness, taking no antibiotics or NSAIDs, and previously screened for no exposure to *A. phagocytophilum* or other pathogen infections. Blood was collected in accordance with the regulations of Human Investigation Committee at Yale University. PMNs were prepared from heparinized human blood as previously described (Thomas and Fikrig, 2007). In brief, red blood cells were sedimented using 6% dextran, lysed with 0.6 M KCl, and the supernatants collected in bulk as white blood cells were layered on Ficoll-Hypaque and further centrifuged. The neutrophil pellets were resuspended in HBSS and infected with cell-free *A. phagocytophilum* obtained from infected HL60 cells and incubated at 37°C at 5% CO$_2$ in RPMI media containing 10% FCS.

Mass spectrometry. Tyrosine phosphorylation of proteins upon *A. phagocytophilum* infection in tick cell line showed induction in proteins that migrated with the molecular masses of ~200 kD (P200), 100 kD (P100), 43 kD (P43), and 25 kD (P25) on 12% SDS-PAGE. The gel spots/bands were excised and characterized by tryptic peptide mass fingerprinting using LC-MS/MS analysis at W.M. Keck Biotechnology Resources at Yale University. This analysis resulted in molecule fragmentation to derive sequences of individual peptides. The data from LC-MS/MS analysis was then analyzed by Mascot search engine for the identification of proteins from primary sequence database. The search parameters also included Phosphorylated Tyrosine. It was searched against the 10/13/2006 NCBInr database. This search revealed that the phosphorylated proteins significantly matched to actin (P43; 14 peptides), α-actinin (P100; 7 peptides), and nonmuscle myosin heavy chain b (P200; eight peptides). Protein sequences and substantial peptide matches corresponding to myosin regulatory light chain (seven peptides), fed tick salivary protein 5 (five peptides), thioredoxin–dependent peroxide reductase (three peptides), and ribosomal protein L18 (two peptides) were identified for band P25.

Immunoblots. Whole cell/nuclear extracts were prepared from uninfected and *A. phagocytophilum*-infected tick cell line or primary cultures of human neutrophils (2 × 10^5 cells). Cells were washed two times with PBS and lysates were prepared with modified RIPA buffer containing protease and phosphatase inhibitors. Whole tick (unfed or 48 h during feeding or after feeding) lysates were prepared by homogenizing the ticks in modified RIPA buffer containing protease and phosphatase inhibitors. Abundant presence of actin in total tick lysate allowed us to analyze the phosphorylated actin without immunoprecipitation. Tick salivary glands and gut extracts were isolated from 48 h during feeding ticks and protein concentrations were determined by Bradford assay (BCA kit). 20 µg of the extracts were resolved on 12% SDS-PAGE and proteins were transferred to nitrocellulose membranes. Actin served as the loading control in most of the immunoblots. Depending on the primary antibodies (actin [Millipore/Cytoskeleton, Inc.], phosphotyrosine/phosphothreonine and PAK1 [Cell Signaling Technologies], phosphoserine/RNAPII/TATA binding protein [Abcam], or P44 [Thomas and Fikrig, 2007] to detect *A. phagocytophilum*), the membrane was incubated with either 5% BSA or milk (according to the manufacturer's instructions) in Tween-20–Tris-buffered saline to bind nonspecific sites. After the primary antibody incubations, immunoblots were treated with either anti–mouse or anti–rabbit HRP-conjugated IgG secondary antibodies based on the manufacturer's instructions (Sigma-Aldrich). Enhanced chemiluminescence detection of antibody binding was performed with the ECL Western blotting detection system (GE Healthcare). Immunoblot films were scanned into jpeg format using a scanner (CanoScan LiDE70; Canon) and images were analyzed and quantified in Photoshop (Adobe) according to the previously described method (Miller et al., 2009; Luhtala and Parker, 2009). The relative intensity of each band on the immunoblots was calculated with respect to the loading controls (total actin or RNAPII) used in the respective experiments. Quantification of all the immunoblots from this study is shown in Table S1.

Genomic DNA Isolation and PCR to detect *A. phagocytophilum* infection. Total genomic DNA was isolated from the mouse peripheral blood or ticks using the DNeasy tissue kit (QIAGEN) according to the manufacturer's protocol. *A. phagocytophilum* burden was determined by analyzing the levels of *P44* gene using Q-PCR as described previously (Sukumaran et al., 2006; Thomas and Fikrig, 2007).

RNA extraction, cDNA synthesis, and Q-RT-PCR analysis. To determine *A. phagocytophilum* burden and tick gene expression, total RNA was extracted with RNeasy extraction kit (QIAGEN) from uninfected or *A. phagocytophilum*–infected tick cells, whole ticks (unfed nymphs/48 h during feeding ticks), mock, *ipak1*-dsRNA–, *ipi3k*-dsRNA–, *igβ*-dsRNA–, or *igγ*-dsRNA–, or inhibitor-injected tick groups. RNA was treated on a column with an RNase-free DNase set (QIAGEN) during isolation to remove contaminating DNA. cDNA was synthesized using the iScript cDNA synthesis kit (Bio-Rad Laboratories). Q-RT-PCR was performed using primers for *A. phagocytophilum P44*, tick genes *salp16*, *salp20*, *salp15*, *salp17*, *salp25D* (Ramamoorthi et al., 2005; Sukumaran et al., 2006; Narasimhan et al., 2007; Thomas and Fikrig, 2007), *ipak1* (5′-CTGATACTGACGGAGA-TTGAGGTGA-3′ and 5′-CATTGTCAGACTTGATGTCCCTGT-3′), *ipi3k* (5′-GCTCTTCAAGTCCGCCCTCA-3′ and 5′-GGACAAACCC-GTGCTTCGT-3′), *igβ* (5′-GGTCCGTTGTTCGCTTTCTCT-3′ and 5′-CACGGTGCACATGTTGTCCA-3′), *igγ* (5′-ATGCACTGCCA-TATGTCCACCT-3′ and 5′-GATGCAGGAGGCTCTTCTCTCGGA-3′), *β tubulin* (5′-CTACGACATCTGCTTCCGCAC-3′ and 5′-GGCGGCCAT-CATGTTCTTG-3′), and *gapdh* (5′-CAGAAGGGCGTTGAGGTCGT-3′ and 5′-CGCCGTCAATGTGCTGCT-3′). Primers for tick *β-actin* cDNA were used in parallel for normalization (Neelakanta et al., 2007). Equal amounts of tick cDNA samples were used in parallel for *β-actin* and *A. phagocytophilum P44* gene Q-RT-PCR analysis.

dsRNA synthesis and tick microinjections. Tick cDNA was prepared and used as template to amplify DNA encoding a fragment of *Ixodes gβ*, *gγ*, *pi3k*,

and pak1. Gene-specific primers containing BglII and KpnI (5′-GAAGATCT-GACGGACGTGGTCTCTGAAACT-3′ and 5′-GGGGTACCGTGGGT-GGCGATGAGGTAGA-3′ for *ipak1*, 5′-GGAAGATCTCAGCTGATC-CGCTTCCCTGA-3′ and 5′-GGGGTACCCCCGCGCACGACTTGA-3′ for *ipi3k*, 5′-GGAAGATCTCTAATTGCACTTACTTGTCCTCCGT-3′ and 5′-GGGGTACCCGCCGCGCAGGTCGT-3′ for *igβ*, and 5′-GGA-AGATCTCTTGCAACAGCAGAGGAAGGT-3′ and 5′-GGGGTA-CCCTCTCGGAATGGGTTCGCCT-3′ for *igγ*) restriction enzyme sites were used in the PCRs. The amplified *Ixodes gβ, gγ, pi3k,* or *pak1* fragments were purified and cloned into the BglII and KpnI sites of the L4440 double T7 Script II vector (Narasimhan et al., 2007). dsRNA complementary to *Ixodes gβ, gγ, pi3k,* or *pak1* sequences were synthesized using the MEGAscript RNAi kit (Applied Biosystems) as described in the user's manual. For acquisition experiments, 3-5 nl *igβ, igγ, ipi3k,* or *ipak1* dsRNA was microinjected into uninfected *I. scapularis* nymphs using glass capillary needle and was inoculated through the idiosoma/body of the ticks into the hemocoel. The feeding and recovery of ticks were performed as described previously (Sukumaran et al., 2006). Ticks in the mock control group were injected with the same volume of dsRNA elution buffer. Ticks were fed on *A. phagocytophilum*–infected mice for the respective time points and analyzed for silencing of *igβ, igγ, ipi3k,* or *ipak1* by Q-RT-PCR.

Inhibitors study. To determine whether inhibition of protein tyrosine phosphatases does further induce actin phosphorylation, uninfected or *A. phagocytophilum*–infected tick cells were treated with 1 mM pervanadate, a protein tyrosine phosphatase inhibitor, for respective times. For pervanadate treatment, we made a stock solution of 100 mM sodium vanadate plus 3% hydrogen peroxide in deionized water. We used inhibitor at 1:100 dilutions when stimulating cells. For PI3K, PAK1, or tyrosine kinase inhibition studies, we infected tick cells with *A. phagocytophilum* and simultaneously treated them with 100 µM of either LY294002 (inhibitor of PI3K) or Genistein (a protein tyrosine kinase inhibitor) or 10 µM of PK-18 (a potent PAK1 inhibitor peptide). Infected cells were treated with similar amounts of DMSO as mock controls. The inhibitors were obtained from EMD and the concentrations of these inhibitors used in this study showed no effects on cell viability as determined by IFA. For tick microinjection studies, 100 µM PI3K or Genistein or 10 µM PAK1 inhibitors were diluted 100× in 10% DMSO and microinjected into the tick body as two hits. Equal amounts of diluted 10% DMSO were microinjected into the mock control ticks and were allowed to recover for 24 h (unfed ticks) or for 3–4 h before feeding on *A. phagocytophilum*–infected mice for acquisition experiment.

PAK1 and PI3K assays. To examine IPAK1 or IPI3K activation, uninfected ticks or uninfected mock injected (buffer alone), or *ipi3k/igβ/igγ*-dsRNA–injected ticks, respectively, were allowed to feed and acquire the bacteria from *A. phagocytophilum*–infected mice. Uninfected ticks that fed on naive mice served as controls. Ticks were collected and snap frozen in liquid nitrogen to arrest the kinase activity. Total lysates or immunoprecipitates from 48 h during feeding ticks were used in all kinase reactions. Whole ticks were either stored frozen at −80°C until use or washed two times with ice-cold PBS and homogenized in ice-cold modified RIPA buffer containing 1% Nonidet P-40, 50 mM Tris, pH 7.5, and 150 mM NaCl supplemented with protease and phosphatase inhibitors. Cleared lysates were preadsorbed with protein A/G agarose beads to block nonspecific binding. Protein amounts were estimated with Bradford assay (BCA kit). Total lysates (250–300 µg) from uninfected or *A. phagocytophilum*–infected and mock control or *ipi3k/igβ/igγ*-silenced ticks were immunoprecipitated overnight at 4°C with PAK1 or PI3K antibodies (Cell Signaling Technologies). Protein A/G agarose beads were incubated for 3–5 h at 4°C to capture the immune complexes. Beads containing immunoprecipitated IPAK1 or IPI3K were washed twice with ice-cold RIPA buffer and three times with respective kinase buffers (50 mM Hepes, pH 7.5, 10 mM MgCl$_2$, 2 mM MnCl$_2$, and 0.2 mM DTT or 50 mM Tris, pH 8, 500 mM NaCl, 5 mM EDTA, 250 µM ATP, and 50 mM MnCl$_2$). IPI3K assays were performed using a kit (Echelon Biosciences, Inc.) where PI was used as substrate in vitro to produce PI(3)P by means of a standard 96-well ELISA format. IPAK1 kinase

assays were performed as previously described (Papakonstanti and Stournaras, 2002) using phosphorylation of the exogenous substrate MBP to assess kinase activity. IPAK1 activity was measured in kinase buffer containing 250 µM ATP (Cell Signaling Technologies) and 20 µg MBP (Millipore) for 30 min at 30°C. Kinase reactions were stopped by the addition of SDS-sample buffer and loading on a 12% SDS-PAGE. Proteins were transferred onto nitrocellulose membranes and probed with phospho-MBP antibody (Millipore), followed by incubation with anti–mouse IgG HRP-conjugated secondary antibody (Sigma-Aldrich). Enhanced chemiluminescence detection of antibody binding was performed with the ECL Western blotting detection system (GE Healthcare).

Rac1/Cdc42 activation assay. Rac1/Cdc42 activation was determined in uninfected and *A. phagocytophilum*–infected ticks collected at 48 h during feeding. The assay was performed with a Rac/Cdc42 activation combo kit (Cell Biolabs, Inc.). In brief, ticks were snap frozen in liquid nitrogen and either stored at −80°C until use or washed two times with ice-cold PBS and homogenized in ice-cold lysis buffer (Rac/Cdc42 activation combo kit; Cell Biolabs, Inc.). Lysates were precleared and proteins were estimated as described before. 250–300 µg of total lysates from uninfected or *A. phagocytophilum*–infected ticks were incubated with PAK-PBD (Rac1/Cdc42 binding domain of PAK1) agarose beads for 1 h. Beads were centrifuged and washed three times with lysis buffer and resuspended in 2× reducing sample buffer and loaded on 12% SDS-PAGE. Proteins were transferred onto nitrocellulose membranes and probed with Rac1 or Cdc42 antibodies (Rac/Cdc42 activation combo kit) followed by incubation with anti-mouse IgG HRP-conjugated secondary antibody. Enhanced chemiluminescence detection was performed as described before.

Mapping of TATA motif in the putative *salp16* and *salp20* promoter regions. The genomic locus corresponding to *salp16* or *salp20* genes were downloaded from http://www.vectorbase.org/ and contigs DS950927 and DS702893 for *salp16* and DS647593, DS772527, and DS916524 for *salp20* were analyzed using SeqMan and DNASTAR software. The genomic region corresponding to −1,000 bp to +100 bp from the start of *salp16* or *salp20* coding sequences was analyzed for putative TATA motifs using three softwares: HCtata, Hamming-Clustering Method for TATA Signal Prediction in Eukaryotic Genes (http://www.itb.cnr.it/sun/webgene/); Neural network promoter prediction (http://www.fruitfly.org/seq_tools/promoter.html); and TSSW recognition of human polymerase II promoter region and start of transcription (www.softberry.com). The results from all the three searches were combined and analyzed for the TATA motif and putative transcription start site. The region that showed TATA motif mapped by all three softwares with high scores was considered for EMSA assays. The region containing TATA motif in putative *salp16* promoter region was PCR amplified using unfed *I. scapularis* genomic DNA as template with oligonucleotides 5′-CTGCGCTGGGATAATCACTTG-3′ and 5′-GACAAA-ATGACATATTCTTACCGAAACA-3′, and TATA motif containing fragment in the *salp20* promoter region was amplified using 5′-CACAAC-TAACCCGTTCAAACTGCT-3′ and 5′-CCGCACAATCCAGAAT-TATTTCT-3′ and sequenced from both the ends.

Biotinylated DNAP assay. Nuclear extracts were prepared from *A. phagocytophilum*–infected ticks (during 48-h engorgement) using the NE-PER Nuclear and Cytoplasmic extraction kit, and extracts were precleared with 50% slurry of streptavidin-coated Sepharose beads (GE Healthcare). Protein amounts were estimated with Bradford assay. 100–200 µg of nuclear extracts was incubated for 30 min at room temperature with 10 µg Poly (dI-dC) for nonspecific binding and 5 µg of site-specific double-stranded biotinylated DNA probes (*salp16* or *salp20*) in gel shift binding buffer (Thermo Fisher Scientific) supplemented with 0.1% NP-40 and 5 mM MgCl$_2$. Biotin-labeled *salp16* or *salp20* probes previously used in EMSA were used in this assay. Streptavidin-coated sepharose beads were incubated for an additional 2 h at 4°C to capture the biotinylated DNA bound to the nuclear extract proteins. Beads were centrifuged and washed twice with ice-cold gel shift binding buffer and twice with PBS and then resuspended in 2× reducing sample buffer,

boiled for 5 min, and loaded on 12% SDS-PAGE. Proteins were transferred onto nitrocellulose membranes and probed with phosphotyrosine or TBP or RNAPII antibodies followed by incubation with anti–mouse IgG HRP-conjugated secondary antibody and enhanced chemiluminescence detection was performed as described before. Total lysates used for immunoprecipitation were probed with actin antibody to serve as the loading control.

Statistical analysis. Statistical significance between the mean values was determined using a nonpaired Student's *t* test. Calculated p-values of <0.05 were considered significant.

Online supplemental material. Fig. S1 shows that *A. phagocytophilum* induces both phosphothreonine and phosphotyrosine phosphorylation of actin in *I. scapularis*. Fig. S2 shows *Ixodes* PAK1 and PI3K sequences. Fig. S3 shows alignments of *Ixodes* PAK1 and PI3K sequences. Fig. S4 shows alignments of *Ixodes* Gβγ subunit sequences. Fig. S5 shows expression and inhibition of *I. scapularis* PAK1, PI3K, Gβ, Gγ, or tyrosine kinases in ticks. Fig. S6 shows that silencing of *ipak*, *ipi3k*, *gβ*, and *gγ* reduces actin phosphorylation in *I. scapularis*. Fig. S7 shows that antibodies against phosphotyrosine, actin, RNAPII, and TBP blocked the band shift with *salp16* probe. Fig. S8 shows a model depicting *A. phagocytophilum*–induced actin phosphorylation in the context of *Ixodes* PI3K–PAK1 signaling, which selectively regulates *salp16* gene transcription. Table S1 shows quantification of Western blots shown in this study. Online supplemental material is available at http://www.jem .org/cgi/content/full/jem.20100276/DC1.

REFERENCES

Bakken, J.S., and S. Dumler. 2008. Human granulocytic anaplasmosis. *Infect. Dis. Clin. North Am.* 22:433–448. doi:10.1016/j.idc.2008.03.011

Bell-Sakyi, L., E. Zweygarth, E.F. Blouin, E.A. Gould, and F. Jongejan. 2007. Tick cell lines: tools for tick and tick-borne disease research. *Trends Parasitol.* 23:450–457.

Bettinger, B.T., D.M. Gilbert, and D.C. Amberg. 2004. Actin up in the nucleus. *Nat. Rev. Mol. Cell Biol.* 5:410–415. doi:10.1038/nrm1370

Bhavsar, A.P., J.A. Guttman, and B.B. Finlay. 2007. Manipulation of host-cell pathways by bacterial pathogens. *Nature.* 449:827–834. doi:10.1038/nature06247

Cameron, L.A., P.A. Giardini, F.S. Soo, and J.A. Theriot. 2000. Secrets of actin-based motility revealed by a bacterial pathogen. *Nat. Rev. Mol. Cell Biol.* 1:110–119. doi:10.1038/35040061

Carlyon, J.A., and E. Fikrig. 2003. Invasion and survival strategies of *Anaplasma phagocytophilum*. *Cell. Microbiol.* 5:743–754. doi:10.1046/j.1462-5822.2003.00323.x

Cossart, P., and A. Toledo-Arana. 2008. *Listeria monocytogenes*, a unique model in infection biology: an overview. *Microbes Infect.* 10:1041–1050. doi:10.1016/j.micinf.2008.07.043

Covacci, A., and R. Rappuoli. 2000. Tyrosine-phosphorylated bacterial proteins: Trojan horses for the host cell. *J. Exp. Med.* 191:587–592. doi:10.1084/jem.191.4.587

Dramsi, S., and P. Cossart. 1998. Intracellular pathogens and the actin cytoskeleton. *Annu. Rev. Cell Dev. Biol.* 14:137–166. doi:10.1146/annurev .cellbio.14.1.137

Dumler, J.S., A.F. Barbet, C.P. Bekker, G.A. Dasch, G.H. Palmer, S.C. Ray, Y. Rikihisa, and F.R. Rurangirwa. 2001. Reorganization of genera in the families *Rickettsiaceae* and *Anaplasmataceae* in the order *Rickettsiales*: unification of some species of *Ehrlichia* with *Anaplasma*, *Cowdria* with *Ehrlichia* and *Ehrlichia* with *Neorickettsia*, descriptions of six new species combinations and designation of *Ehrlichia equi* and 'HGE agent' as subjective synonyms of *Ehrlichia phagocytophila*. *Int. J. Syst. Evol. Microbiol.* 51:2145–2165.

Dumler, J.S., K.S. Choi, J.C. Garcia-Garcia, N.S. Barat, D.G. Scorpio, J.W. Garyu, D.J. Grab, and J.S. Bakken. 2005. Human granulocytic anaplasmosis and *Anaplasma phagocytophilum*. *Emerg. Infect. Dis.* 11:1828–1834.

Frischknecht, F., S. Cudmore, V. Moreau, I. Reckmann, S. Röttger, and M. Way. 1999a. Tyrosine phosphorylation is required for actin-based motility of *vaccinia* but not *Listeria* or *Shigella*. *Curr. Biol.* 9:89–92. doi:10.1016/S0960-9822(99)80020-7

Frischknecht, F., V. Moreau, S. Röttger, S. Gonfloni, I. Reckmann, G. Superti-Furga, and M. Way. 1999b. Actin-based motility of *vaccinia* virus mimics receptor tyrosine kinase signalling. *Nature.* 401:926–929. doi:10.1038/44860

Galisteo, M.L., J. Chernoff, Y.C. Su, E.Y. Skolnik, and J. Schlessinger. 1996. The adaptor protein Nck links receptor tyrosine kinases with the serine-threonine kinase Pak1. *J. Biol. Chem.* 271:20997–21000. doi:10.1074/jbc.271.35.20997

Gerisch, G., A.A. Noegel, and M. Schleicher. 1991. Genetic alteration of proteins in actin-based motility systems. *Annu. Rev. Physiol.* 53:607–628. doi:10.1146/annurev.ph.53.030191.003135

Goldberg, M.B. 2001. Actin-based motility of intracellular microbial pathogens. *Microbiol. Mol. Biol. Rev.* 65:595–626. doi:10.1128/MMBR.65.4 .595-626.2001

Goosney, D.L., D.G. Knoechel, and B.B. Finlay. 1999. Enteropathogenic *E. coli*, *Salmonella*, and *Shigella*: masters of host cell cytoskeletal exploitation. *Emerg. Infect. Dis.* 5:216–223. doi:10.3201/eid0502.990205

Gouin, E., C. Egile, P. Dehoux, V. Villiers, J. Adams, F. Gertler, R. Li, and P. Cossart. 2004. The RickA protein of *Rickettsia conorii* activates the Arp2/3 complex. *Nature.* 427:457–461. doi:10.1038/nature02318

Gouin, E., M.D. Welch, and P. Cossart. 2005. Actin-based motility of intracellular pathogens. *Curr. Opin. Microbiol.* 8:35–45. doi:10.1016/j.mib.2004.12.013

Hodzic, E., D. Fish, C.M. Maretzki, A.M. De Silva, S. Feng, and S.W. Barthold. 1998. Acquisition and transmission of the agent of human granulocytic ehrlichiosis by *Ixodes scapularis* ticks. *J. Clin. Microbiol.* 36:3574–3578.

Hofmann, W.A. 2009. Cell and molecular biology of nuclear actin. *Int Rev Cell Mol Biol.* 273:219–263. doi:10.1016/S1937-6448(08)01806-6

Hofmann, W.A., and P. de Lanerolle. 2006. Nuclear actin: to polymerize or not to polymerize. *J. Cell Biol.* 172:495–496. doi:10.1083/jcb .200601095

Hofmann, W.A., L. Stojiljkovic, B. Fuchsova, G.M. Vargas, E. Mavrommatis, V. Philimonenko, K. Kysela, J.A. Goodrich, J.L. Lessard, T.J. Hope, et al. 2004. Actin is part of pre-initiation complexes and is necessary for transcription by RNA polymerase II. *Nat. Cell Biol.* 6:1094–1101. doi:10 .1038/ncb1182

IJdo, J.W., A.C. Carlson, and E.L. Kennedy. 2007. *Anaplasma phagocytophilum* AnkA is tyrosine-phosphorylated at EPIYA motifs and recruits SHP-1 during early infection. *Cell. Microbiol.* 9:1284–1296. doi:10.1111/j.1462-5822.2006.00871.x

Jungbluth, A., V. von Arnim, E. Biegelmann, B. Humbel, A. Schweiger, and G. Gerisch. 1994. Strong increase in the tyrosine phosphorylation of actin upon inhibition of oxidative phosphorylation: correlation with reversible rearrangements in the actin skeleton of *Dictyostelium* cells. *J. Cell Sci.* 107:117–125.

Jungbluth, A., C. Eckerskorn, G. Gerisch, F. Lottspeich, S. Stocker, and A. Schweiger. 1995. Stress-induced tyrosine phosphorylation of actin in *Dictyostelium* cells and localization of the phosphorylation site to tyrosine-53 adjacent to the DNase I binding loop. *FEBS Lett.* 375:87–90. doi:10.1016/0014-5793(95)01165-B

Katavolos, P., P.M. Armstrong, J.E. Dawson, and S.R. Telford III. 1998. Duration of tick attachment required for transmission of granulocytic ehrlichiosis. *J. Infect. Dis.* 177:1422–1425. doi:10.1086/517829

Lin, M., A. den Dulk-Ras, P.J. Hooykaas, and Y. Rikihisa. 2007. *Anaplasma phagocytophilum* AnkA secreted by type IV secretion system is tyrosine

phosphorylated by Abl-1 to facilitate infection. *Cell. Microbiol.* 9:2644–2657. doi:10.1111/j.1462-5822.2007.00985.x

Liu, X., S. Shu, M.S. Hong, R.L. Levine, and E.D. Korn. 2006. Phosphorylation of actin Tyr-53 inhibits filament nucleation and elongation and destabilizes filaments. *Proc. Natl. Acad. Sci. USA.* 103:13694–13699. doi:10.1073/pnas.0606321103

Luhtala, N., and R. Parker. 2009. LSM1 over-expression in *Saccharomyces cerevisiae* depletes U6 snRNA levels. *Nucleic Acids Res.* 37:5529–5536. doi:10.1093/nar/gkp572

Martinez, J.J., and P. Cossart. 2004. Early signaling events involved in the entry of *Rickettsia conorii* into mammalian cells. *J. Cell Sci.* 117:5097–5106. doi:10.1242/jcs.01382

McCarty, J.H. 1998. The Nck SH2/SH3 adaptor protein: a regulator of multiple intracellular signal transduction events. *Bioessays.* 20:913–921. doi:10.1002/(SICI)1521-1878(199811)20:11<913::AID-BIES6>3.0.CO;2-T

Menard, R.E., and R.R. Mattingly. 2004. Gbetagamma subunits stimulate p21-activated kinase 1 (PAK1) through activation of PI3-kinase and Akt but act independently of Rac1/Cdc42. *FEBS Lett.* 556:187–192. doi:10.1016/S0014-5793(03)01406-6

Miller, R.K., H. Qadota, T.J. Stark, K.B. Mercer, T.S. Wortham, A. Anyanful, and G.M. Benian. 2009. CSN-5, a component of the COP9 signalosome complex, regulates the levels of UNC-96 and UNC-98, two components of M-lines in *Caenorhabditis elegans* muscle. *Mol. Biol. Cell.* 20:3608–3616. doi:10.1091/mbc.E09-03-0208

Münter, S., M. Way, and F. Frischknecht. 2006. Signaling during pathogen infection. *Sci. STKE.* 2006:re5. doi:10.1126/stke.3352006re5

Narasimhan, S., B. Sukumaran, U. Bozdogan, V. Thomas, X. Liang, K. DePonte, N. Marcantonio, R.A. Koski, J.F. Anderson, F. Kantor, and E. Fikrig. 2007. A tick antioxidant facilitates the Lyme disease agent's successful migration from the mammalian host to the arthropod vector. *Cell Host Microbe.* 2:7–18. doi:10.1016/j.chom.2007.06.001

Navarro, L., A. Koller, R. Nordfelth, H. Wolf-Watz, S. Taylor, and J.E. Dixon. 2007. Identification of a molecular target for the *Yersinia* protein kinase A. *Mol. Cell.* 26:465–477. doi:10.1016/j.molcel.2007.04.025

Neelakanta, G., X. Li, U. Pal, X. Liu, D.S. Beck, K. DePonte, D. Fish, F.S. Kantor, and E. Fikrig. 2007. Outer surface protein B is critical for *Borrelia burgdorferi* adherence and survival within *Ixodes* ticks. *PLoS Pathog.* 3:e33. doi:10.1371/journal.ppat.0030033

Papakonstanti, E.A., and C. Stournaras. 2002. Association of PI-3 kinase with PAK1 leads to actin phosphorylation and cytoskeletal reorganization. *Mol. Biol. Cell.* 13:2946–2962. doi:10.1091/mbc.02-01-0599

Park, J., K.J. Kim, K.S. Choi, D.J. Grab, and J.S. Dumler. 2004. *Anaplasma phagocytophilum* AnkA binds to granulocyte DNA and nuclear proteins. *Cell. Microbiol.* 6:743–751. doi:10.1111/j.1462-5822.2004.00400.x

Patel, J.C., and J.E. Galán. 2005. Manipulation of the host actin cytoskeleton by *Salmonella*—all in the name of entry. *Curr. Opin. Microbiol.* 8:10–15. doi:10.1016/j.mib.2004.09.001

Patel, J.C., K. Hueffer, T.T. Lam, and J.E. Galán. 2009. Diversification of a *Salmonella* virulence protein function by ubiquitin-dependent differential localization. *Cell.* 137:283–294. doi:10.1016/j.cell.2009.01.056

Pawson, T., and J.D. Scott. 2005. Protein phosphorylation in signaling—50 years and counting. *Trends Biochem. Sci.* 30:286–290. doi:10.1016/j.tibs.2005.04.013

Pederson, T., and U. Aebi. 2002. Actin in the nucleus: what form and what for? *J. Struct. Biol.* 140:3–9. doi:10.1016/S1047-8477(02)00528-2

Pedra, J.H., S. Narasimhan, D. Rendic, K. Deponte, L. Bell-Sakyi, I.B. Wilson, and E. Fikrig. 2010. Fucosylation enhances colonization of ticks by *Anaplasma phagocytophilum. Cell. Microbiol.*

Percipalle, P., and N. Visa. 2006. Molecular functions of nuclear actin in transcription. *J. Cell Biol.* 172:967–971. doi:10.1083/jcb.200512083

Pollard, T.D., and G.G. Borisy. 2003. Cellular motility driven by assembly and disassembly of actin filaments. *Cell.* 112:453–465. doi:10.1016/S0092-8674(03)00120-X

Ramamoorthi, N., S. Narasimhan, U. Pal, F. Bao, X.F. Yang, D. Fish, J. Anguita, M.V. Norgard, F.S. Kantor, J.F. Anderson, et al. 2005. The Lyme disease agent exploits a tick protein to infect the mammalian host. *Nature.* 436:573–577. doi:10.1038/nature03812

Sansonetti, P. 2002. Host-pathogen interactions: the seduction of molecular cross talk. *Gut.* 50:III2–III8. doi:10.1136/gut.50.suppl_3.iii2

Schwan, T.G. 1996. Ticks and *Borrelia*: model systems for investigating pathogen-arthropod interactions. *Infect. Agents Dis.* 5:167–181.

Selbach, M., F.E. Paul, S. Brandt, P. Guye, O. Daumke, S. Backert, C. Dehio, and M. Mann. 2009. Host cell interactome of tyrosine-phosphorylated bacterial proteins. *Cell Host Microbe.* 5:397–403. doi:10.1016/j.chom.2009.03.004

Sells, M.A., U.G. Knaus, S. Bagrodia, D.M. Ambrose, G.M. Bokoch, and J. Chernoff. 1997. Human p21-activated kinase (Pak1) regulates actin organization in mammalian cells. *Curr. Biol.* 7:202–210. doi:10.1016/S0960-9822(97)70091-5

Sells, M.A., J.T. Boyd, and J. Chernoff. 1999. p21-activated kinase 1 (Pak1) regulates cell motility in mammalian fibroblasts. *J. Cell Biol.* 145:837–849. doi:10.1083/jcb.145.4.837

Stevens, J.M., E.E. Galyov, and M.P. Stevens. 2006. Actin-dependent movement of bacterial pathogens. *Nat. Rev. Microbiol.* 4:91–101. doi:10.1038/nrmicro1320

Sukumaran, B., S. Narasimhan, J.F. Anderson, K. DePonte, N. Marcantonio, M.N. Krishnan, D. Fish, S.R. Telford, F.S. Kantor, and E. Fikrig. 2006. An *Ixodes scapularis* protein required for survival of *Anaplasma phagocytophilum* in tick salivary glands. *J. Exp. Med.* 203:1507–1517. doi:10.1084/jem.20060208

Thomas, V., and E. Fikrig. 2007. *Anaplasma phagocytophilum* specifically induces tyrosine phosphorylation of ROCK1 during infection. *Cell. Microbiol.* 9:1730–1737. doi:10.1111/j.1462-5822.2007.00908.x